JAM3 maintains leukemia-initiating cell self-renewal through LRP5/AKT/β-catenin/CCND1 signaling

Yaping Zhang,[1] Fangzhen Xia,[1] Xiaoye Liu,[1] Zhuo Yu,[1] Li Xie,[1] Ligen Liu,[1] Chiqi Chen,[1] Haishan Jiang,[1] Xiaoxin Hao,[1] Xiaoxiao He,[1] Feifei Zhang,[1] Hao Gu,[1] Jun Zhu,[2] Haitao Bai,[2] Cheng Cheng Zhang,[3] Guo-Qiang Chen,[1] and Junke Zheng[1]

[1]Department of Pathophysiology, Key Laboratory of Cell Differentiation and Apoptosis of Chinese Ministry of Education, Hongqiao International Institute of Medicine, Shanghai Tongren Hospital/Faculty of Basic Medicine, Shanghai Jiao Tong University School of Medicine, Shanghai, China. [2]Department of Hematology, First People's Hospital, Shanghai Jiao Tong University School of Medicine, Shanghai, China. [3]Department of Physiology, UT Southwestern Medical Center, Dallas, Texas, USA.

Leukemia-initiating cells (LICs) are responsible for the initiation, development, and relapse of leukemia. The identification of novel therapeutic LIC targets is critical to curing leukemia. In this report, we reveal that junctional adhesion molecule 3 (JAM3) is highly enriched in both mouse and human LICs. Leukemogenesis is almost completely abrogated upon *Jam3* deletion during serial transplantations in an MLL-AF9–induced murine acute myeloid leukemia model. In contrast, *Jam3* deletion does not affect the functions of mouse hematopoietic stem cells. Moreover, knockdown of *JAM3* leads to a dramatic decrease in the proliferation of both human leukemia cell lines and primary LICs. JAM3 directly associates with LRP5 to activate the downstream PDK1/AKT pathway, followed by the downregulation of GSK3β and activation of β-catenin/CCND1 signaling, to maintain the self-renewal ability and cell cycle entry of LICs. Thus, JAM3 may serve as a functional LIC marker and play an important role in the maintenance of LIC stemness through unexpected LRP5/PDK1/AKT/GSK3β/β-catenin/CCND1 signaling pathways but not via its canonical role in cell junctions and migration. JAM3 may be an ideal therapeutic target for the eradication of LICs without influencing normal hematopoiesis.

Introduction

Acute myeloid leukemia (AML) is one of the most common malignant hematopoietic disorders in adults and may originate from hematopoietic stem cells (HSCs) or their downstream progenitors with the accumulation of different genetic mutations. Leukemia-initiating cells (LICs) are considered to be responsible for the initiation, development, and relapse of leukemia. Because traditional strategies, such as chemotherapy or radiotherapy, cannot completely eliminate the LICs in the bone marrow (BM) niche, leukemia relapse often occurs after treatment. Although BM transplantation can cure leukemia, the difficulties in obtainment of MHC-matched donor HSCs sometimes hamper its application in the clinic. Recently, several lines of evidence have shown that leukemia could potentially be efficiently eradicated using either blocking antibodies specific to certain surface (immune) molecules or chimeric antigen receptor T (CAR-T) cells (1–4). These surface molecules may also receive extrinsic regulatory signals provided by the BM special "niche" to control intrinsic genetic programs essential for LIC function. Therefore, the identification of other surface molecules specific for LIC stemness is important for screening/developing functional blocking antibodies, small-molecule chemicals, or CAR-T cells for the elimination of leukemia.

Recently, studies from our and other groups have demonstrated that several surface molecules, including leukocyte immunoglobulin-like receptor subfamily B member 2 (LILRB2) (5), CD123 (6), Tie2 (7), CD47 (3, 4), and CD93 (8), are required for the maintenance of LIC stemness and may be attractive targets for leukemia treatment. We further revealed that the high-affinity ligand of LILRB2, angiopoietin-like protein member 2 (ANGPLT2), exists in exosomes and may be involved in the activities of both HSCs and LICs (9). These findings led us to speculate that other surface (immune) molecules may be required for hematopoiesis or leukemogenesis. It is also possible that some surface molecules are indispensable only for LICs but not for normal HSCs, which will serve as the LIC functional markers and ideal targets for leukemia treatment. To this end, we screened a number of surface molecules using the MLL-AF9–induced human primary AML cells (MA9 cells; ref. 10) or patients' samples, and revealed that several candidates are highly expressed on MA9 cells or LICs, including BTLA, CD244, JAM3, B7-H1, and B7-H4. Our subsequent study indicated that B7-H1 is also important for leukemogenesis (11). However, the functions of other surface molecules in leukemogenesis remain largely unknown.

Interestingly, we observed that JAM3, which mainly functions as an adhesion molecule, is also highly expressed on LICs, indicating that it may be required for the leukemogenesis. So far, 5 junctional adhesion molecules (JAMs) have been identified: JAM1–JAM4 and JAML (12). JAMs belong to the immunoglobulin superfamily and play important roles in the maintenance of tight junction integrity, regulation of cell migration, and determination of cellular polarity (13–15). JAM3 is expressed on several types of cells, such as epithelial cells (16), spermatids (17), neuronal stem

Authorship note: YZ, FX, XL, and ZY contributed equally to this work.
Conflict of interest: The authors have declared that no conflict of interest exists.
Submitted: February 3, 2017; **Accepted:** February 8, 2018.
Reference information: *J Clin Invest*. 2018;128(5):1737–1751.
https://doi.org/10.1172/JCI93198.

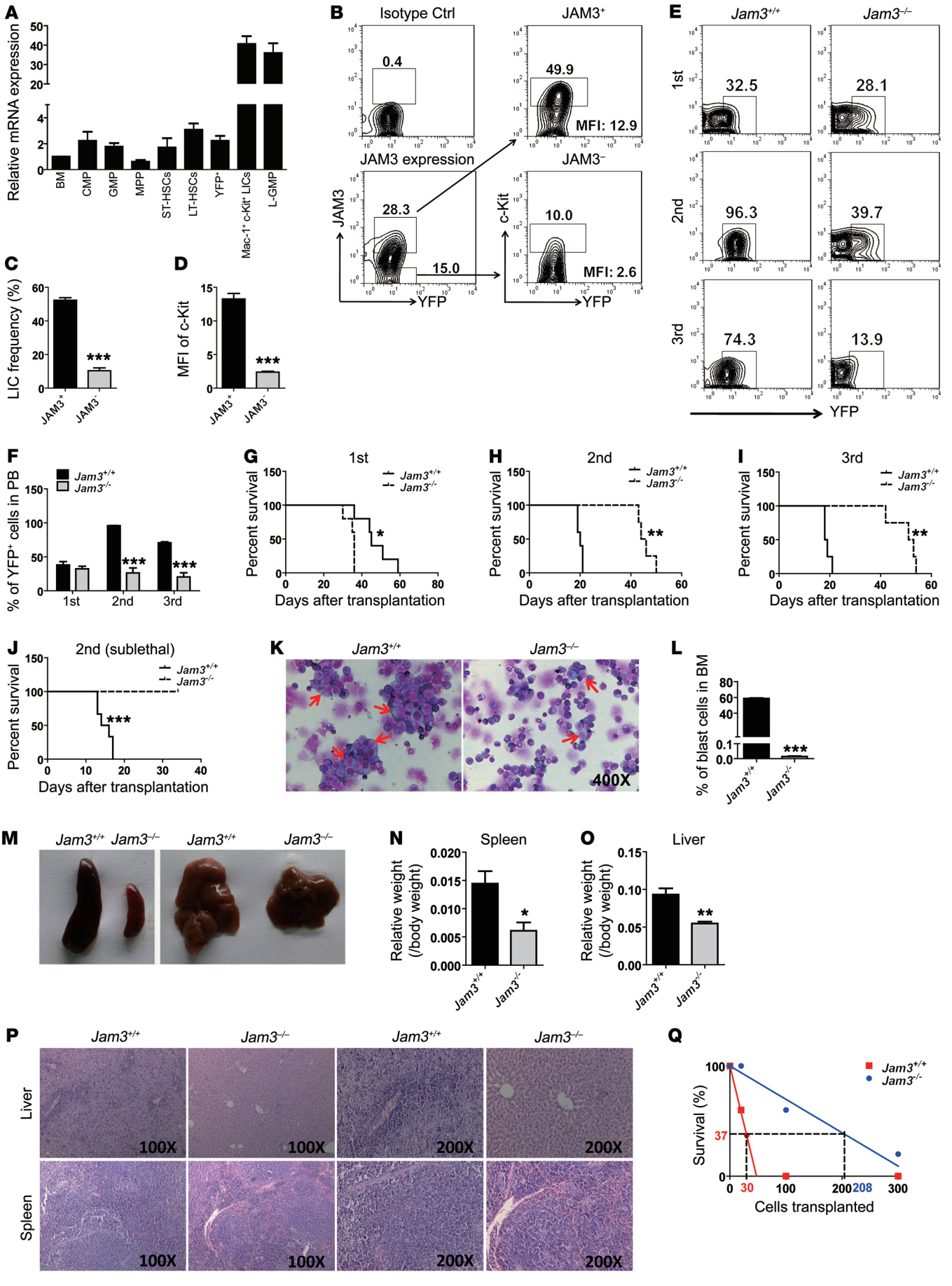
A
Relative mRNA expression
BM
CMP
GMP
MPP
ST-HSCs
LT-HSCs
YFP+
Mac-1+ c-Kit+ LICs
L-GMP
B
Isotype Ctrl
JAM3+
0.4
49.9
MFI: 12.9
JAM3 expression
JAM3−
28.3
15.0
10.0
MFI: 2.6
JAM3
c-Kit
YFP
C
LIC frequency (%)
JAM3+
JAM3−
D
MFI of c-Kit
E
Jam3+/+
Jam3−/−
1st
2nd
3rd
32.5
28.1
96.3
39.7
74.3
13.9
YFP
F
% of YFP+ cells in PB
G
1st
H
2nd
I
3rd
Percent survival
Days after transplantation
J
2nd (sublethal)
K
400X
L
% of blast cells in BM
M
N
Spleen
Relative weight (/body weight)
O
Liver
P
100X
200X
Q
Survival (%)
Cells transplanted

Figure 1. JAM3 is highly enriched in LICs and required for their self-renewal abilities. (**A**) mRNA levels of JAM3 in total BM cells, CMP, GMP, MPP, ST-HSCs, LT-HSCs, YFP$^+$ leukemia cells, YFP$^+$Mac-1$^+$c-Kit$^+$ LICs, and L-GMP cells was measured by quantitative RT-PCR (n = 3). (**B**–**D**) MLL-AF9$^+$ leukemia cells were evaluated for LIC frequencies and c-Kit expression levels (MFI) in JAM3$^+$ and JAM3$^-$ cells (n = 3; ***P < 0.001, Student's t test). (**E**) Representative flow cytometric analysis of leukemia cells in the peripheral blood of recipient mice receiving transplants of WT or *Jam3*-null MLL-AF9$^+$ BM cells upon the first to third transplantation. (**F**) Quantification data in **E** (n = 4–5; ***P < 0.001, 2-way ANOVA followed by Bonferroni's post-test). PB, peripheral blood. (**G**–**I**) Survival data for recipient mice (lethally irradiated) receiving WT or *Jam3*-null MLL-AF9$^+$ BM cells upon the first (**G**), second (**H**), and third transplantation (**I**) (n = 4–5; *P < 0.05, **P < 0.01, log-rank test). (**J**) Survival data for recipient mice (sublethally irradiated) receiving WT or *Jam3*-null leukemia cells upon the second transplantation (n = 5; ***P < 0.001, log-rank test). (**K**) Representative images of Giemsa-Wright staining for WT and *Jam3*-null MLL-AF9$^+$ BM cells upon the second transplantation. (**L**) Quantification of the frequencies of blast cells in **K** (n = 3; ***P < 0.001, Student's t test). (**M**) Representative images of the sizes of spleens and livers of recipient mice upon the second transplantation. (**N** and **O**) Quantification of the weight of spleens and livers in **M** (n = 4; *P < 0.05, **P < 0.01, Student's t test). (**P**) Histological H&E staining of livers and spleens. (**Q**) Limiting dilution assays comparing the frequencies of LICs in WT and *Jam3*-null MLL-AF9$^+$ BM cells. Experiments were conducted 3–5 times for validation.

cells (18), and cancer cells (i.e., lung cancer, ref. 13; ovarian tumors, ref. 19; melanoma, ref. 20; and lymphoma cells, ref. 21), and is involved in many physiological or pathological activities. Recently, JAM3 has also been reported to be expressed on both murine HSCs and progenitor cells. Intriguingly, JAM3 deletion does not affect the stemness of HSCs but leads to a significantly increased frequency of myeloid progenitor cells in the BM (22). However, the distribution and function of JAM3 on LICs remain unknown, which prompted us to study the roles of JAM3 in leukemogenesis.

JAM3 has 2 extracellular Ig-like domains and a cytoplasmic tail with a PDZ binding motif (23), which can interact with PAR-3, PAR-6, ZO-1, PATJ, and PICK-1 to participate in the formation of polarity complexes or other activities (17, 24, 25). JAM3 homotypically (26) or heterotypically interacts with the integrin Mac-1 (27), JAM2 (16), and the viral receptor CAR (28) to enhance the homing, proliferation, or metastasis of cancer cells. Blocking JAM3 with an antibody also suppressed angiogenesis and tumor growth in a mouse lung cancer model (29). Administration of anti-JAM3 monoclonal antibodies effectively inhibits the development of lymphoma through the suppression of ERK1/2 signaling (30). Nevertheless, whether JAM3 regulates leukemia development through similar or other signaling mechanisms requires further investigation.

In this study, we demonstrate that JAM3 is highly expressed in mouse LICs and plays a unique role in the self-renewal of LICs. JAM3 can serve as a functional marker for LICs. Loss of JAM3 results in cell cycle arrest at the G_1-S transition of LICs and dramatically delayed leukemia development. JAM3 interacts with LRP5 to activate the PDK1/AKT pathway, which remarkably enhances β-catenin/CCND1 activities to maintain the stemness of LICs.

Results

JAM3 is highly enriched in LICs and required for their self-renewal abilities. To understand the roles of JAM3 in LICs, we first examined the expression of JAM3 in a murine MLL-AF9–induced (tagged with yellow fluorescent protein [YFP]) AML model. The forced expression of MLL-AF9 in HSCs/progenitor cells usually results in leukemogenesis within 4 weeks. These AML cells only expressed myeloid cell markers (Mac-1 and Gr-1), not lymphoid cell markers (CD3 and B220; Supplemental Figure 1, A–C; supplemental material available online with this article; https://doi.org/10.1172/JCI93198DS1), as previously described (5, 31). To determine whether there was any difference of *Jam3* expression levels between leukemogenesis and normal hematopoiesis, we measured the *Jam3* transcript expression in total leukemia bulk cells (YFP$^+$) and their comparable counterparts of normal BM cells, or immunophenotypic YFP$^+$Mac-1$^+$c-Kit$^+$ LICs initially reported by Somervaille and Cleary (31) and their comparable counterparts of Lin$^-$Sca-1$^+$c-Kit$^+$CD34$^-$Flk2$^-$ HSCs, using quantitative reverse transcriptase PCR (RT-PCR). Interestingly, the level of *Jam3* in mouse YFP$^+$Mac-1$^+$c-Kit$^+$ LICs was approximately 45-, 15-, or 13-fold higher than those in the normal BM cells, HSCs, or YFP$^+$ BM leukemia cells, respectively (Figure 1A). *Jam3* transcript was also measured in different hematopoietic/myeloid compartments, including long-term HSCs (LT-HSCs), short-term HSCs (ST-HSCs), multipotent progenitors (MPPs), common myeloid progenitors (CMPs), and granulocyte-monocyte progenitors (GMPs), which showed that LT-HSCs had a slightly higher level of *Jam3* expression than ST-HSCs, MPPs, CMPs, and GMPs (Figure 1A). Since some groups (such as Scott Armstrong's group, ref. 32) have revealed that LICs are enriched in Lin$^-$IL7R$^-$Sca-1$^-$c-Kit$^+$CD34$^+$FcR-II/III$^+$ L-GMP cells, we also measured the *Jam3* transcript in L-GMP cells and found that they had an expression level of *Jam3* similar to that of YFP$^+$Mac-1$^+$c-Kit$^+$ LICs, which was around 16- and 18-fold greater than those of normal LT-HSCs and GMP, respectively (Figure 1A). Moreover, although only 30% of AML cells were positive for JAM3 expression (Figure 1B), this population contains approximately 5.0-fold more immunophenotypic LICs (52.3% vs. 10.4%; Figure 1C) and expressed approximately 5.6-fold higher intensities of the LIC marker c-Kit compared with JAM3$^-$ cells (mean fluorescence intensity [MFI], 13.3 vs. 2.4; Figure 1D). Consistently, LICs had much higher percentages of JAM3$^+$ cells than mature leukemia cells (41.3% vs. 14.6%; Supplemental Figure 1, D and E). These unique characteristics of JAM3 caused us to further study its functions in LICs.

Using WT and *Jam3*-knockout mice (*Jam3*$^{+/+}$ and *Jam3*$^{-/-}$ hereafter), we then examined the frequencies of WT and *Jam3*-null YFP$^+$ leukemia cells of primary recipient mice, which showed no significant differences in the peripheral blood 3 weeks after transplantation (Figure 1, E and F). Surprisingly, the recipients receiving *Jam3*-null cells had slightly reduced survival time compared with their WT counterparts (36 vs. 45 days; Figure 1G), although the LIC frequencies from both peripheral blood and BM (Supplemental Figure 1, F–H) and the weight and infiltration of the leukemic livers or spleens were not significantly altered between these 2 groups (Supplemental Figure 1, I and J). We speculated that the decreased survival in *Jam3*-null primary recipient mice might be caused by the increased frequency of *Jam3*-null myeloid progenitors as previously described (22). To further pinpoint the functions of JAM3 in LICs, we performed serial transplantation with the same number of AML cells and found that *Jam3*-null YFP$^+$ leukemia cells in peripheral blood were markedly decreased compared with WT controls after both the second and third transplantations (39.7% vs. 96.3% and 13.9% vs. 74.1%, respectively; Figure 1, E and

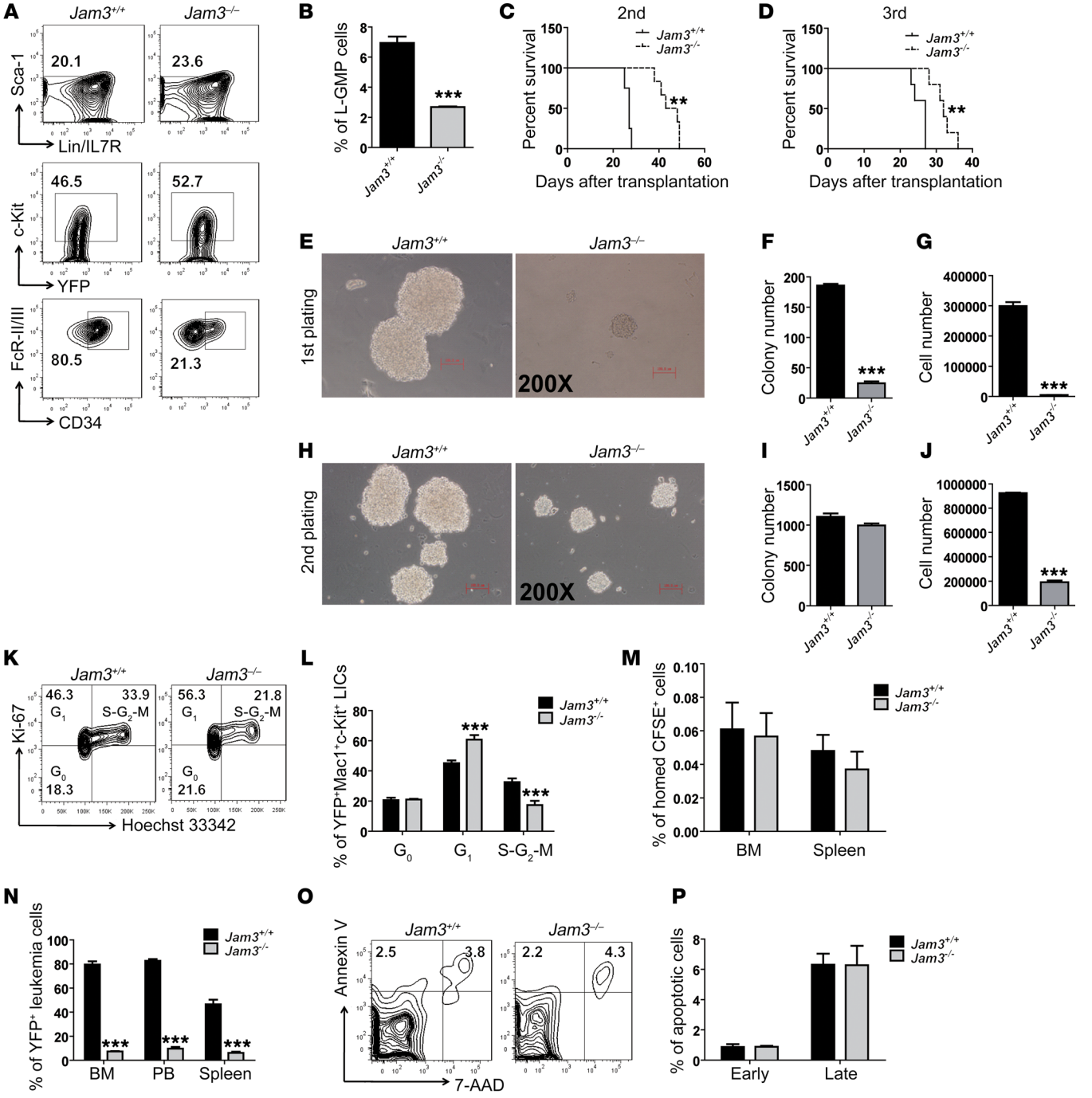

Figure 2. JAM3 promotes the self-renewal of LICs through enhanced cell cycle entry. (**A**) Representative flow cytometric analysis for WT and *Jam3*-null L-GMP cells of the recipients upon the secondary transplantation. (**B**) Quantification of frequencies of L-GMP cells in **A** (n = 3; ***P < 0.001, Student's t test). (**C** and **D**) Survival data for recipient mice receiving WT or *Jam3*-null L-GMP cells upon the second to third transplantation (n = 5; **P < 0.01, log-rank test). (**E**–**G**) Representative images of colony formation of WT and *Jam3*-null YFP$^+$Mac-1$^+$c-Kit$^+$ LICs of the secondary recipients in the first plating (**E**). The colony numbers (**F**) and total cell numbers of colonies in **E** (**G**) were counted (n = 3; ***P < 0.001, Student's t test). (**H**–**J**) Representative images of colony formation of WT and *Jam3*-null leukemia cells clonogenically derived from the first plating (**H**). The colony numbers (**I**) and total cell numbers of colonies in **H** (**J**) were calculated (n = 3; ***P < 0.001, Student's t test). (**K**) Cell cycle status was determined in WT and *Jam3*-null YFP$^+$Mac-1$^+$c-Kit$^+$ LICs of the secondary recipients. (**L**) Quantitative analysis of the cell cycle distribution in **K** (n = 4–6; ***P < 0.001, 2-way ANOVA followed by Bonferroni's post-test). (**M**) CFSE-labeled WT and Jam3-null leukemia cells of secondary recipients were transplanted and analyzed for the homed CFSE$^+$ cells in the recipients' BM and spleen (n = 5–6). (**N**) WT and *Jam3*-null leukemia cells of secondary recipients were transplanted into the recipient mice by intratibial injection, followed by the examination of leukemia cells 2 weeks later (n = 5; ***P < 0.001, Student's t test). (**O**) Representative flow cytometric analysis of apoptosis of WT or *Jam3*-null YFP$^+$Mac-1$^+$c-Kit$^+$ LICs. (**P**) Quantification of data in **O** (n = 4). Experiments were conducted 3–5 times for validation.

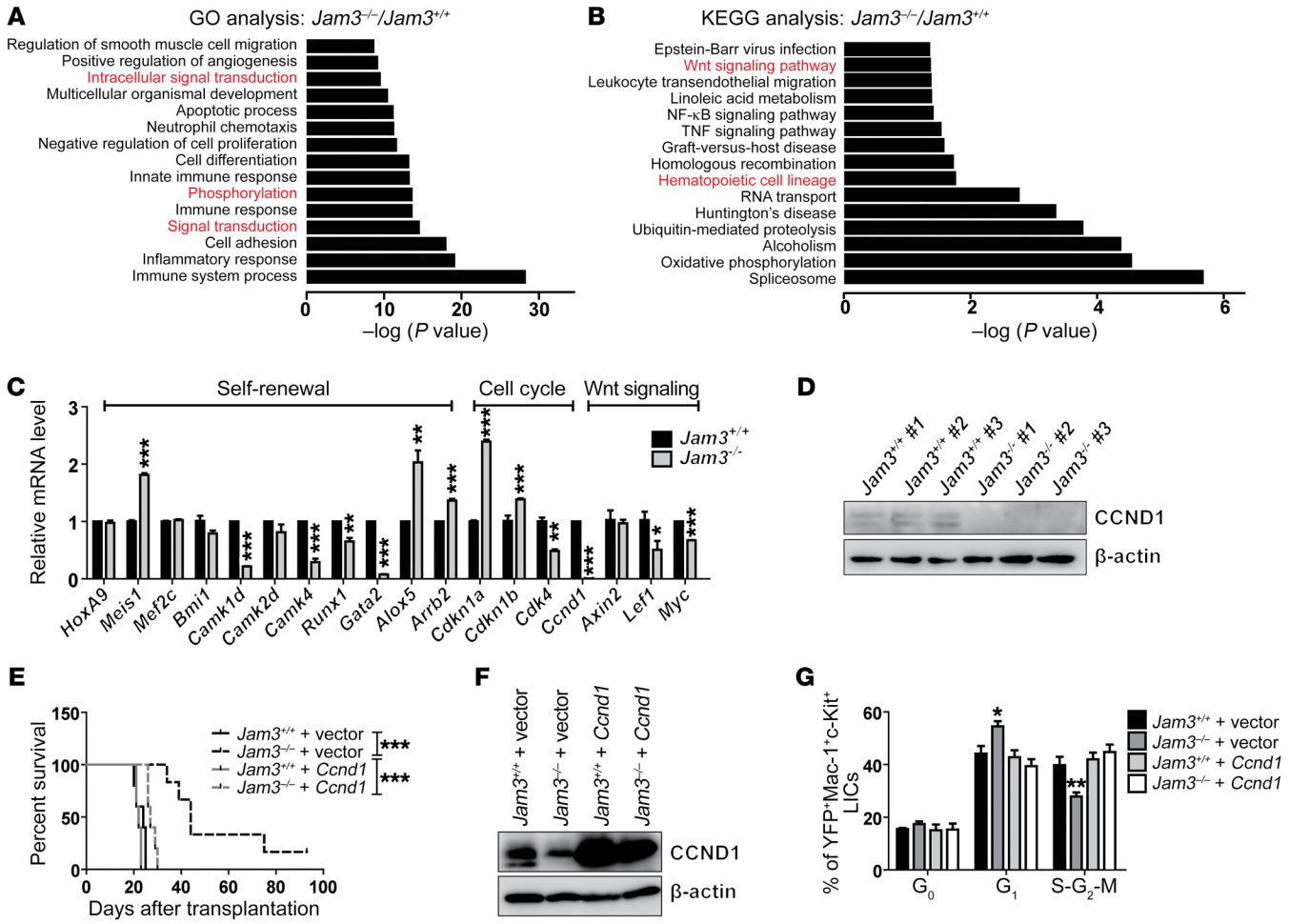

Figure 3. JAM3 maintains the CCND1 level to promote the self-renewal of LICs. (**A** and **B**) GO (biological process) and KEGG (pathway) analyses of the microarray data of WT or *Jam3*-null YFP$^+$Mac-1$^+$c-Kit$^+$ LICs. Candidate changes are highlighted in red. (**C**) Potential candidates related to self-renewal, cell cycle, and Wnt signaling were examined in WT and *Jam3*-null LICs by quantitative RT-PCR (n = 3; $^*P < 0.05$, $^{**}P < 0.01$, $^{***}P < 0.001$, Student's t test). (**D**) CCND1 levels were compared between WT and *Jam3*-null YFP$^+$Mac-1$^+$c-Kit$^+$ LICs by immunoblotting. (**E**) *Ccnd1* was ectopically expressed in *Jam3*-null leukemia cells and injected into recipient mice. Survival was compared among the mice receiving WT cells, *Jam3*-null cells, and *Ccnd1*-overexpressing WT or *Jam3*-null cells (n = 5–6; $^{***}P < 0.001$, log-rank test). (**F**) CCND1 levels were validated in leukemia cells from the rescue experiment in **E**. (**G**) The cell cycle distribution in YFP$^+$Mac-1$^+$c-Kit$^+$ LICs from the rescue experiment in **E** was determined using Ki-67 and Hoechst 33342 staining (n = 3–5; $^*P < 0.05$, $^{**}P < 0.01$, 2-way ANOVA followed by Bonferroni's post-test). Experiments were conducted 3–5 times for validation.

F). Consistently, recipient mice receiving *Jam3*-null leukemia cells had remarkably delayed survival times during the subsequent serial transplantation (45 vs. 20 days and 52 vs. 18.5 days for the second and third transplantation, respectively; Figure 1, H and I). More strikingly, the development of leukemia was completely abolished when primary leukemia cells were injected into sublethally irradiated recipient mice (Figure 1J).

Meanwhile, Giemsa-Wright staining displayed a significantly lower frequency of the *Jam3*-null blast cells in the BM compared with WT controls upon secondary transplantation (Figure 1, K and L), which was consistent with a notable decrease in the sizes/relative weight of spleens and livers of *Jam3*-null leukemic recipient mice (Figure 1, M–O). The histological H&E staining also revealed much less infiltration in the recipient mice injected with *Jam3*-null leukemia cells (Figure 1P). More importantly, the LIC frequencies were further determined in WT and *Jam3*-null leukemia cells of secondary recipient mice by a limiting dilution analysis, which showed that the deletion of *Jam3* resulted in an 85.6% decrease in the functional LICs compared with the WT counterparts (1 in 208 vs. 1 in 30; Figure 1Q and Supplemental Table 1).

Moreover, we also used 2 other leukemia models, the AML1-ETO9a–induced M2 AML model (33) and the N-Myc–induced B cell acute lymphoid leukemia model (34) (B-ALL), to test whether JAM3 plays a specific role in certain types of leukemia. As shown in Supplemental Figure 1, K–O, although *Jam3* transcript was expressed in both AML1-ETO9a$^+$ and N-Myc$^+$ leukemia cells as determined by quantitative RT-PCR, recipient mice receiving *Jam3*-null AML1-ETO9a$^+$ AML cells, but not N-Myc$^+$ B-ALL cells, had significantly extended survival during serial transplantation. In contrast, we found that JAM3 had no effect on normal hematopoiesis, as evaluated by a competitive transplantation (Supplemental Figure 1, P and Q), which is consistent with previously reported data (22). Interestingly, no significant changes of HSC self-renewal and differentiation abilities were found in *Jam3*-null

HSCs upon serial transplantation (Supplemental Figure 1, R–U). Taken together, these data suggest that JAM3 is required to maintain the self-renewal ability of LICs, but not HSCs, which indicates that JAM3 may be an ideal target for LICs. Because we observed that the self-renewal ability was dramatically reduced upon the second or third transplantation, we mainly focused on the phenotypes in secondary recipient mice for subsequent studies.

JAM3 promotes the self-renewal of LICs through enhanced cell cycle entry. To further understand how JAM3 maintains the self-renewal of LICs, the frequency of YFP$^+$Mac-1$^+$c-Kit$^+$ LICs was analyzed in the BM of the secondary recipient mice. Surprisingly, we did not observe significantly different WT and *Jam3*-null LIC frequencies (Supplemental Figure 2, A and B). Because the Lin$^-$IL7R$^-$Sca-1$^-$c-Kit$^+$CD34$^+$FcR-II/III$^+$ L-GMP population has been suggested to be another, more stringent way to determine the immunophenotypic LICs, we measured the L-GMP cell frequency and demonstrated that the percentage of *Jam3*-null L-GMP cells was markedly reduced compared with the WT population (Figure 2, A and B). More importantly, the median leukemia latency in *Jam3*-null L-GMP cells from both primary and secondary recipient mice was significantly extended (Figure 2, C and D), indicating that JAM3 is indispensable for the self-renewal abilities of LICs. Interestingly, a surrogate functional analysis with methylcellulose medium in vitro showed that the clonogenic potential of *Jam3*-null YFP$^+$Mac-1$^+$c-Kit$^+$ LICs was almost completely abolished, as indicated by the remarkable reduction in both the colony number and total cell number during primary plating (colony number, 188 vs. 24; cell number, 3.0×10^5 vs. 0.5×10^5; Figure 2, E–G). The secondary plating with clonogenically derived leukemia cells further revealed a marked decrease in colony size and total cell number, although the colony number was only slightly reduced (Figure 2, H–J). These data also suggest that *Jam3*-null YFP$^+$Mac-1$^+$c-Kit$^+$ LICs have severe functional defects, although the LIC percentage is similar to WT counterparts (Supplemental Figure 2, A and B).

Several lines of evidence indicate that LICs may exist in a nonquiescent population of cells controlled by certain cyclins or other cell cycle regulators, such as CCND2 (35). Recently, Iwasaki et al. provided interesting data and showed that CD93 marks nonquiescent human LICs by controlling their self-renewal through the inhibition of CDKN2B (8). These studies prompted us to analyze the cell cycle status in *Jam3*-null LICs by Ki-67/Hoechst 33342 staining, which demonstrated that there was a remarkably increased frequency of *Jam3*-null LICs in G_1 phase in comparison with WT controls (60.8% vs. 45.2%), but a 30% decrease in the S-G_2-M fraction (Figure 2, K and L). Similar changes in the cell cycle distribution were found using Pyronin Y/Hoechst 33342 staining (Supplemental Figure 2, C and D). Moreover, to understand whether the cell cycle phenotype starts after transplantation or soon after MLL-AF9 is expressed, we examined the cell cycle status at different time points during primary transplantation. We did not find any cell cycle changes between WT and *Jam3*-null LICs 48 hours after MLL-AF9 transduction (Supplemental Figure 2, E and F) or 2 weeks after transduction/transplantation (Supplemental Figure 2G). However, G_1 cell cycle arrest could be detected 4 weeks after transplantation (Supplemental Figure 2H), indicating that cell cycle phenotype starts after transplantation or during the late stage of proliferation/self-renewal of LICs in vivo, which is further enhanced upon serial transplantation. These results also suggest that the reduced self-renewal ability upon *Jam3* deletion may be caused by the dysregulation of certain cell cycle regulators.

Since many studies have reported that JAM3 plays a role in cell-cell interaction by interplaying with certain unknown soluble or membrane-bound molecules (27, 36, 37), JAM3 may interact with stromal cells in the BM niche to regulate LIC activities. To address this possibility, we then performed experiments by culturing YFP$^+$Mac-1$^+$c-Kit$^+$ LICs with the BM stromal cell line OP9-DL1 in either normoxic or hypoxic conditions (1% O_2) to mimic BM niche. Although a 1.5- or 2.0-fold increase in cell number from WT LICs was observed when cultured without stromal cells in normoxic or hypoxic conditions, respectively, a 4- or 4.5-fold greater cell number was found upon coculture with OP9-DL1 cells compared with that of *Jam3*-null cells (Supplemental Figure 2, I, J, M). Similarly, this coculture system revealed that WT LICs gave rise to many more colonies than their counterparts in both conditions (Supplemental Figure 2, K, L, and N). These data indicate that stromal cells may be involved in the cell-cell interaction and support leukemia growth in vivo.

Because JAM3 has also been reported to be a key adhesion molecule in controlling cell migration and adhesion, to exclude the possibility that defective LIC migration or adhesion contributes to the effects of *Jam3* loss, we first analyzed the homing ability of *Jam3*-null leukemia cells. Surprisingly, there was no significant difference in the frequencies of WT and *Jam3*-null CFSE-labeled total BM leukemia cells that homed to the BM or spleen 16 hours after injection (Figure 2M and Supplemental Figure 2O). Furthermore, a total of 2×10^6 YFP$^+$Mac-1$^+$c-Kit$^+$ LICs were injected into the lethally irradiated mice, followed by analyses of the homed cells in spleens and BM at 6, 12, and 18 hours after transplantation. However, no significant differences in homing abilities were found between WT and *Jam3*-null LICs (Supplemental Figure 2, P and Q). To further test whether JAM3 controls the migration of LICs out of the BM, *Jam3*-null leukemia cells were transplanted into recipient mice by intratibial injection, followed by the detection of YFP$^+$ leukemia cells in the BM, peripheral blood, and spleen. Similarly, the frequencies of leukemia cells were simultaneously reduced in all the tested tissues (Figure 2N). *Jam3* deletion also had no effect on the migration and adhesion abilities of LICs as evaluated by in vitro Transwell assay (Supplemental Figure 2R) and OP9-DL1 cell–mediated adhesion analysis (Supplemental Figure 2S), respectively. Together with the homing analyses, these results clearly show that JAM3 does not affect the migration and adhesion ability of LICs. JAM3 also had no effect on the apoptosis or differentiation of LICs, as evaluated by annexin V and 7-aminoactinomycin D (7-AAD) staining (Figure 2, O and P) or flow cytometric analyses of the Gr-1 expression levels on BM leukemia cells (Supplemental Figure 2, T and U). Thus, JAM3 is mainly required for the G_1-S transition but not for migration, adhesion, apoptosis, and differentiation, which contributes to the self-renewal of LICs and leukemia development.

JAM3 maintains the CCND1 level to promote the self-renewal of LICs. To unravel the underlying molecular mechanisms that control the self-renewal and cell cycle arrest in *Jam3*-null LICs, WT and *Jam3*-null LICs were subjected to microarray analyses. Because we mainly found that *Jam3* deletion led to the loss of self-renewal and

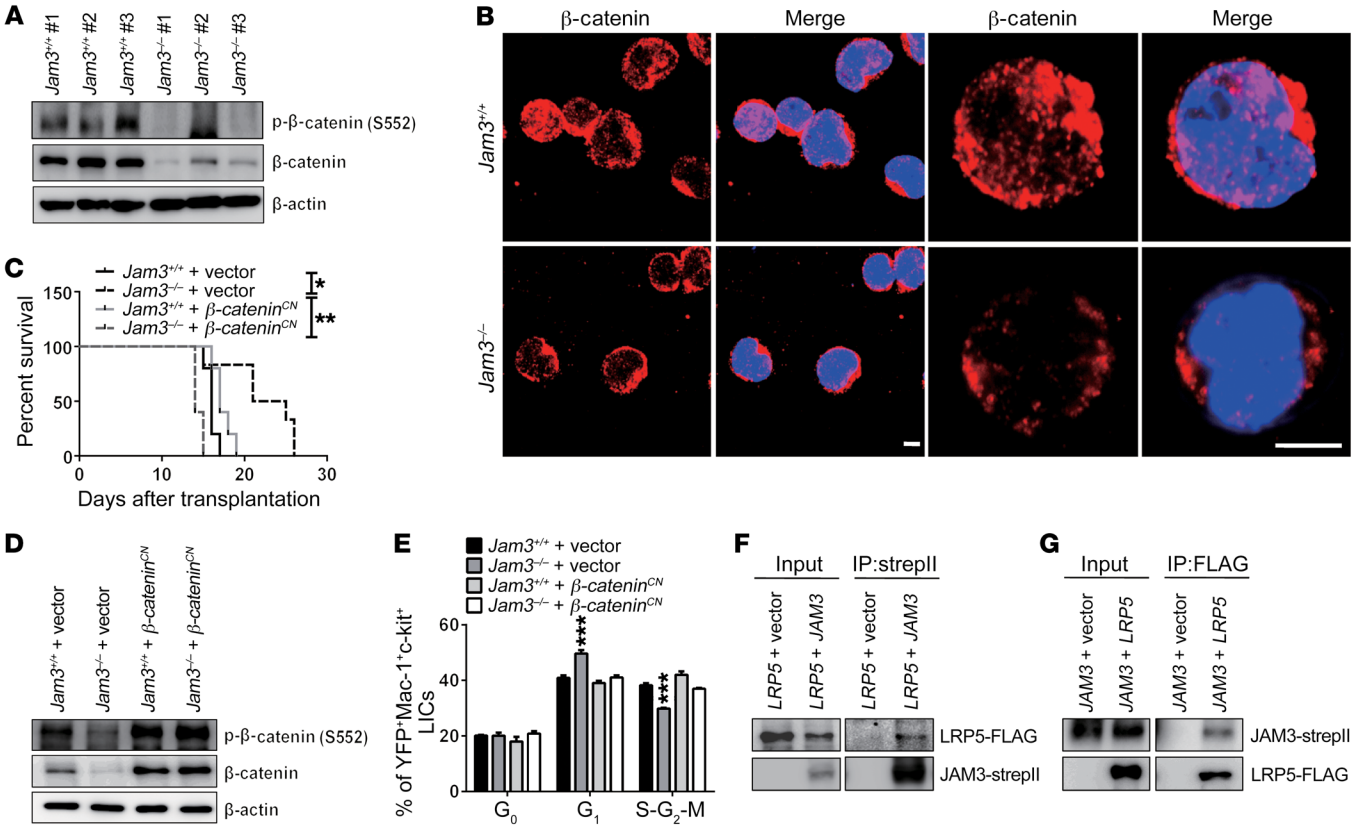

Figure 4. JAM3 collaborates with LRP5 to activate β-catenin/CCND1 signaling. (**A**) Phospho–β-catenin (S552) and total β-catenin levels were evaluated between WT and *Jam3*-null YFP$^+$Mac-1$^+$c-Kit$^+$ LICs by immunoblotting. (**B**) β-Catenin levels were compared between WT and *Jam3*-null YFP$^+$Mac-1$^+$c-Kit$^+$ LICs by immunofluorescence staining. Scale bars: 5 μm. (**C**) A constitutively active form of phospho–β-catenin (S37A, *β-catenin^{CN}*) was subcloned in the pCDH-EF1a-T2A-mCherry vector and ectopically expressed in *Jam3*-null leukemia cells, which were then injected into recipient mice. Survival was compared among the mice receiving WT cells, *Jam3*-null cells, and *β-catenin^{CN}*–overexpressing WT or *Jam3*-null cells (n = 5–6; *P < 0.05, **P < 0.01, log-rank test). (**D**) Phospho–β-catenin (S552) and total β-catenin levels were validated in leukemia cells from the rescue experiment in **C**. (**E**) The cell cycle distribution in YFP$^+$Mac-1$^+$c-Kit$^+$ LICs from the rescue experiment in **C** was determined using Ki-67 and Hoechst 33342 staining (n = 3; ***P < 0.001, 2-way ANOVA followed by Bonferroni's post-test). (**F**) StrepII-tagged *JAM3* and FLAG-tagged *LRP5* were overexpressed in 293T cells, and their lysates were coimmunoprecipitated by strepII beads, followed by Western blotting analysis for FLAG (LRP5). (**G**) A reverse coimmunoprecipitation experiment was performed after LRP5-FLAG pull-down, followed by Western blotting analysis for strepII (JAM3). The empty vector was used as the control. Experiments were conducted 3 times for validation.

cell cycle changes of LICs, we first focused on the signal pathways that might be involved in self-renewal and cell cycle regulation, such as signal transduction and phosphorylation pathways in Gene Ontology (GO) analysis (Figure 3A) and Wnt signaling and hematopoietic cell lineage in Kyoto Encyclopedia of Genes and Genomes (KEGG) analysis (Figure 3B), and consistently demonstrated that several such related genes (*Mef2c*, *Bmi1*, *Camk1d*, *Camk4*, and *Gata2* for self-renewal; *Cdk4* and *Ccnd1* for cell cycle; *Ccnd1*, *Fzd4*, and *Myc* for Wnt signaling) were notably reduced in *Jam3*-null LICs compared with WT controls (Supplemental Figure 3A). On the other side, we did not observe notable difference in migration or cell adhesion (Figure 2N and Supplemental Figure 2, P and Q) and apoptosis (Figure 2, O and P), which promoted us to speculate that the changes in migration, cell adhesion, or apoptosis in GO or NF-κB pathway in KEGG might not be important for the *Jam3*-null phenotype. Meanwhile, given that the mice were lethally irradiated and the immune system was destroyed before transplantation, and little evidence supported that JAM3 was important for immune response, we believed that the immune response in GO or TNF pathway in KEGG also might not be the potential candidate.

We then validated the mRNA expression levels of these candidates by quantitative RT-PCR and demonstrated that *Camk1d*, *Camk4*, *Gata2*, and *Ccnd1* transcripts were markedly downregulated (Figure 3C), indicating that they may be downstream targets of *Jam3*. Because *Ccnd1* serves as a key cell cycle regulator for the G_1-S transition and is one of the downstream targets of Wnt signaling, which is also consistent with the G_1 phase arrest and downregulation of Wnt signaling in *Jam3*-null LICs (Figure 2, K and L, and Figure 3B), it is very likely that *Ccnd1* is a potential target of *Jam3*. Consistent with a 99% reduction in the mRNA level of *Ccnd1*, Western blotting analysis also showed that the CCND1 protein level was almost completely abolished in *Jam3*-null LICs (Figure 3D). *Ccnd1* was then ectopically expressed in *Jam3*-null leukemia cells, which were then injected into recipient mice. As shown in Figure 3, E and F, the recipient mice receiving *Ccnd1*-overexpressing *Jam3*-null AML cells had markedly reduced survival compared with mice injected with *Jam3*-null control cells, which was comparable to the WT counterparts. In contrast, the overexpression of *Ccnd1* had no influence on the WT leukemia cells (Figure 3E), indicating that the physiological protein level of CCND1 is critical to maintain the stemness of

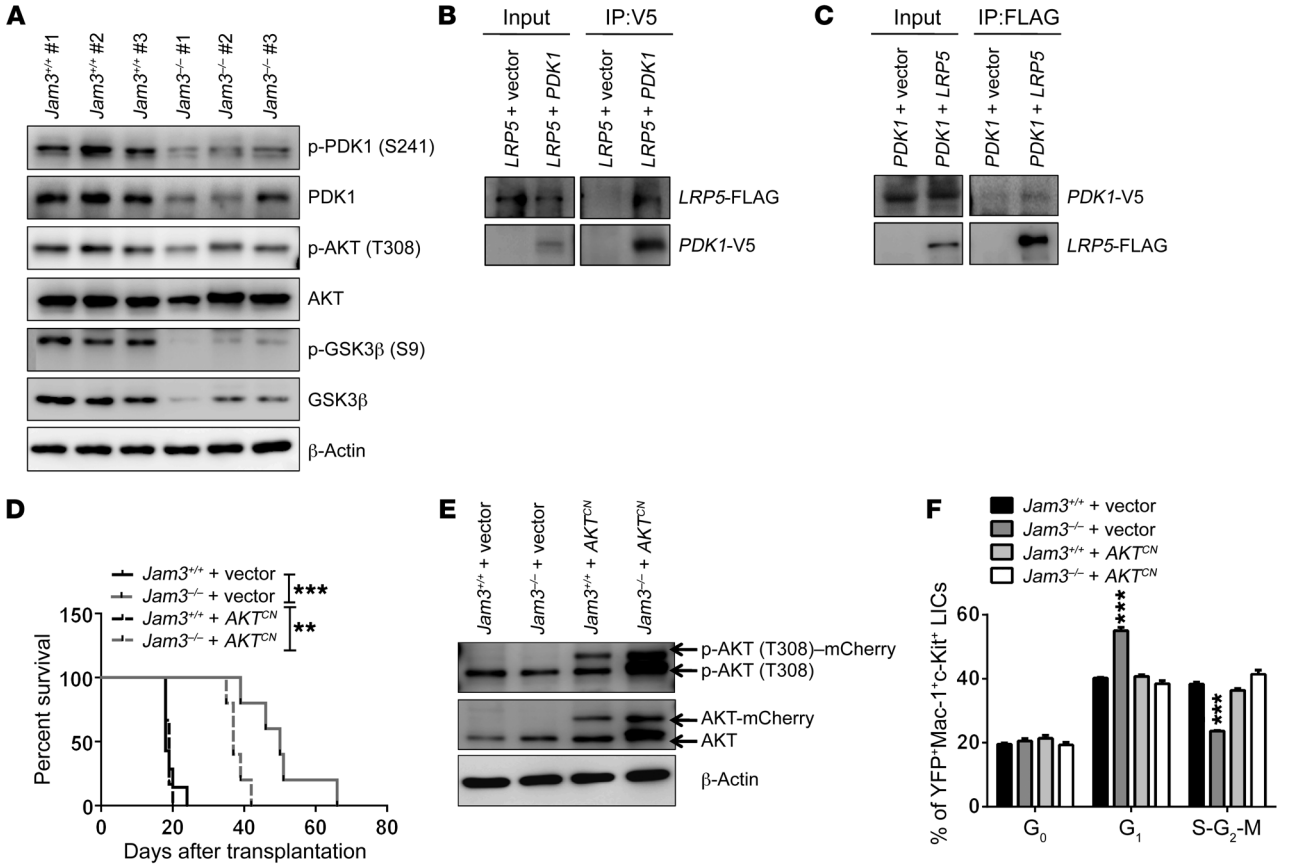

Figure 5. LRP5 interacts with PDK1 to activate AKT signaling to inhibit GSK3β. (**A**) Protein levels of phospho-PDK1 (S241), PDK1, phospho-AKT (T308), AKT, phospho-GSK3β (S9), and GSK3β were measured in WT and *Jam3*-null YFP$^+$Mac-1$^+$c-Kit$^+$ LICs by immunoblotting. (**B**) V5-tagged *PDK1* and FLAG-tagged *LRP5* were overexpressed in 293T cells, and their lysates were coimmunoprecipitated by V5 antibodies and protein A/G beads, followed by Western blotting analysis for FLAG (LRP5). (**C**) A reverse coimmunoprecipitation experiment was performed after LRP5-FLAG pull-down, followed by Western blotting analysis for PDK1 (V5). (**D**) A constitutively active form of phospho-*AKT* (E17K, *AKT^{CN}*) was subcloned into pCDH-EF1a-T2A-mCherry vector and ectopically expressed in *Jam3*-null leukemia cells, followed by injection into recipient mice. Survival was compared among the mice receiving WT cells, *Jam3*-null cells, and *AKT^{CN}*-overexpressing WT or *Jam3*-null cells (n = 5–7; $^{**}P < 0.01$, $^{***}P < 0.001$, log-rank test). (**E**) Phospho-AKT (T308) and AKT levels were validated in leukemia cells from the rescue experiment in **D**. (**F**) The cell cycle distribution in YFP$^+$Mac-1$^+$c-Kit$^+$ LICs from the rescue experiment in **D** was determined using Ki-67 and Hoechst 33342 staining (n = 3; $^{***}P < 0.001$, 2-way ANOVA followed by Bonferroni's post-test). The empty vector was used as the control. Experiments were conducted 3 times for validation.

LICs. Moreover, the G_1 phase arrest in *Jam3*-null LICs could be fully reversed upon the overexpression of *Ccnd1* (Figure 3G). In contrast, overexpression of *Camk1d*, *Camk4*, or *Gata2* in *Jam3*-null leukemia cells could not rescue the loss of *Jam3* functions in vivo (Supplemental Figure 3B). Therefore, these results reveal that JAM3 interplays with CCND1 signaling to regulate the self-renewal of LICs.

JAM3 collaborates with LRP5 to activate β-catenin/CCND1 signaling. *Ccnd1*, *Lef1*, and *Myc*, 3 main downstream target genes of Wnt signaling, were remarkably decreased in *Jam3*-null LICs (Figure 3C), indicating that the Wnt pathway may be involved in JAM3 functions during leukemogenesis. We further examined the protein level of the key upstream regulator, β-catenin, in *Jam3*-null LICs by Western blotting, which showed that the levels of both phosphorylated and total β-catenin were strikingly reduced (Figure 4A). This was consistent with an increased level of cytoplasmic β-catenin in *Jam3*-null LICs, as evaluated by immunofluorescence staining (Figure 4B). Moreover, overexpression of a constitutively active form of *β-catenin* (S37A, *β-catenin^{CN}*) in *Jam3*-null leukemia cells could fully reverse the extended survival time but had no effect on WT leukemia cells (Figure 4C). The ectopically expressed levels of *β-catenin* were confirmed by immunoblotting (Figure 4D and Supplemental Figure 4, A and B). Similarly to *Ccnd1*, overexpression of *β-catenin^{CN}* was also able to reverse the G_1-S transition arrest, as measured by Ki-67/Hoechst 33342 staining (Figure 4E).

To determine how JAM3 influences the protein level of β-catenin, coimmunoprecipitation experiments were performed to test whether JAM3 was directly associated with the Wnt receptors and coreceptors, such as LRP5, FZD1, and FZD4. Interestingly, LRP5, but not FZD1, FZD4, or other candidate receptors, could be detected when JAM3 was pulled down (Figure 4F and data not shown). Conversely, JAM3 could be detected upon LRP5 pull-down (Figure 4G). These results suggest that JAM3 interacts with LRP5 to promote β-catenin activation and translocation into the nucleus to activate downstream targets. In addition, it seems that JAM3 can also stabilize the protein level of β-catenin.

LRP5 interacts with PDK1 to activate AKT signaling to inhibit GSK3β activities. To further understand how JAM3 affects the β-catenin/CCND1 pathway, we further examined the level of

a key upstream regulator, GSK3β, by immunoblotting, showing that both inactive phospho-GSK3β (Ser9) and the total protein level were markedly reduced in *Jam3*-null LICs (Figure 5A). Since AKT signaling can directly inhibit the activities of GSK3β through enhanced phosphorylation of Ser9, we then examined the changes in AKT signaling as well as its upstream regulator PDK1. Strikingly, the phosphorylation of both AKT (T308) and PDK1 (S241) was notably reduced in *Jam3*-null LICs (Figure 5A). Meanwhile, the total protein level of PDK1, but not AKT, was also slightly decreased (Figure 5A). The decreased PDK1/AKT signaling prompted us to examine whether JAM3 also interacts with the PDK1/AKT pathway. Surprisingly, no direct interaction was found between JAM3 and PDK1 or AKT as evaluated by coimmunoprecipitation experiments (Supplemental Figure 4, C and D). Then, we thought that there may be an association between LRP5 and PDK1, and eventually demonstrated that LRP5 could be immunoprecipitated upon PDK1 pull-down (Figure 5B). Conversely, PDK1 could be detected upon LRP5 pull-down (Figure 5C).

To further determine whether the activation of AKT signaling could reverse the phenotypes of *Jam3*-null LICs, a constitutively active form of AKT (E17K, AKT^{CN}) was overexpressed in *Jam3*-null leukemia cells, which were then injected into recipient mice. Intriguingly, the recipient mice receiving AKT^{CN}-overexpressing *Jam3*-null cells had significantly reduced survival time, which was comparable to the WT mice (Figure 5D). In contrast, AKT^{CN} overexpression did not affect the survival of WT leukemic mice (Figure 5D). The ectopic expression levels of AKT^{CN} were confirmed by Western blot analysis (Figure 5E and Supplemental Figure 4, E and F). As expected, the G_1 arrest in *Jam3*-null LICs was fully reversed upon the constitutive activation of AKT signaling, as measured by Ki-67/Hoechst 33342 staining (Figure 5F). These results reveal that JAM3 is associated with LRP5, which directly interacts with PDK1 to enhance the downstream AKT signaling to suppress the GSK3β level, followed by the activation of β-catenin/CCND1 signaling in LICs. Moreover, we constructed a JAM3 chimeric reporter, similar to what we described in a previous study (38), to confirm that anti-JAM3 antibody (39, 40) indeed could bind to the JAM3 expressed on the surface of reporter cells, although the binding affinity seemed to be very low since only 10% of reporter cells were activated upon the antibody stimulation (Supplemental Figure 5A). Nevertheless, the treatment with JAM3 antibody led to a slightly, but significantly, extended survival of the recipient mice compared with the control ones (Supplemental Figure 5B), indicating that it may be possible to efficiently eliminate LICs by targeting JAM3 with high-affinity JAM3 antibody.

JAM3 is required for the proliferation of human AML cell lines. To further evaluate the functions of JAM3 in human AML, we first measured the protein levels of JAM3 on different types of human AML cell lines by flow cytometric analysis. As shown in Figure 6A, several AML cell lines indeed expressed JAM3, including Kasumi-1 (M2), HL-60 (M3), THP-1 (M5), U937 (M5), and MV4-11 (M5). We further decided to construct shRNAs to knock down *JAM3* to test its roles in these cell lines. As shown in Figure 6B, all 4 shRNAs (sh1188, sh997, sh359, and sh731), especially sh1188, could efficiently downregulate the protein levels of JAM3 in *JAM3*-overexpressing 293T cells, as evaluated by immunoblotting. We then knocked down the expression of *JAM3* in THP-1 cells with sh1188 and revealed that these cells expanded much more slowly compared with those infected with the scrambled shRNA (Figure 6, C and D). Consistently, sh731 had less of an effect on the proliferation of THP-1 cells because of its reduced *JAM3* knockdown efficiency (Figure 6B). We observed a similar effect on the growth in other AML cell lines, such as U937, Kasumi-1, and HL-60, after the knockdown of *JAM3* (Figure 6, E–G). A functional assay further showed that *JAM3*-knockdown THP-1 cells gave rise to far fewer colonies in vitro (Figure 6, H and I). Mechanistically, *JAM3*-knockdown THP-1 cells exhibited an enlarged cell size (Supplemental Figure 6, A and B) and tended to arrest in G_1 phase, as determined by BrdU incorporation analysis (Figure 6, J and K). The blockage of the cell cycle might also lead to a significant increase in apoptosis (Supplemental Figure 6, C and D).

We also examined JAM3-mediated pathways in different types of human AML cell lines, including THP-1 (with MLL-AF9 fusion, M5), U937 (without MLL-AF9 fusion, M5), Kasumi-1 (without MLL-AF9 fusion, M2), and HL-60 (without MLL-AF9 fusion, M3), which showed that JAM3/PDK1/AKT/β-catenin/CCND1 pathways were significantly reduced in all 4 tested cell lines (Supplemental Figure 6E). These results suggest that JAM3-mediated signaling is not specific to MLL-AF9 fusion, but is required for the leukemogenesis of several types of AML with or without MLL-AF9 fusion (at least for M2, M3, and M5 AMLs as we examined herein) rather than for B-ALL (Supplemental Figure 1, N and O). Consistently, overexpression of *JAM3* in THP-1 cells could significantly enhance PDK1/AKT/β-catenin/CCND1 signaling (Supplemental Figure 6F). And knockdown of *LRP5* in THP-1 cells led to a marked downregulation of PDK1/AKT/β-catenin/CCND1 signaling, which could efficiently reverse the enhanced signaling resulting from the *JAM3* overexpression (Supplemental Figure 6F). Consistently, a high level of JAM3 resulted in a 4- to 6-fold increase of total cell numbers after in vitro culture for 6 days (Supplemental Figure 6, G and H), or 3-fold more colonies as evaluated with the methylcellulose medium (Supplemental Figure 6, I and J). However, the enhanced growth rate, as well as the colony-forming ability, was almost fully abrogated when *LRP5* was simultaneously silenced in *JAM3*-overexpressing THP-1 cells (Supplemental Figure 6, G–J). These functional experiments revealed that LRP5 is required for JAM3-mediated pathways.

JAM3 supports the growth of human acute myeloid LICs. To further test the role of JAM3 in human LICs, we examined the expression levels of *JAM3* on human primary LICs of several M2 (2 cases, AML#6 and AML#8) and M5 AML samples (3 cases, AML#2, AML#5, and AML#7) with or without MLL-AF9 fusion (Supplemental Table 2) using flow cytometric analysis, which showed that JAM3 was enriched only in $Lin^-CD34^+CD38^-CD90^-CD45RA^+$ LMPP cells (LIC-enriched cell population) and not in other $CD34^-CD38^-$ differentiated leukemia cells, as indicated by both frequencies and MFIs in different samples (Figure 7, A–C). Consistently, we observed that human $Lin^-CD34^+CD38^-CD90^-CD45RA^+$ LMPP cells had much higher levels of *JAM3* transcripts than the $CD34^-CD38^-$ differentiated leukemia cells, their normal counterpart LMPP cells, or $Lin^-CD34^+CD38^-CD90^+CD45RA^-$ HSCs (Supplemental Figure 7A). In silico analyses were performed with data extracted from the curated BloodSpot database (http://servers.binf.ku.dk/bloodspot/; NCBI Gene Expression Omnibus

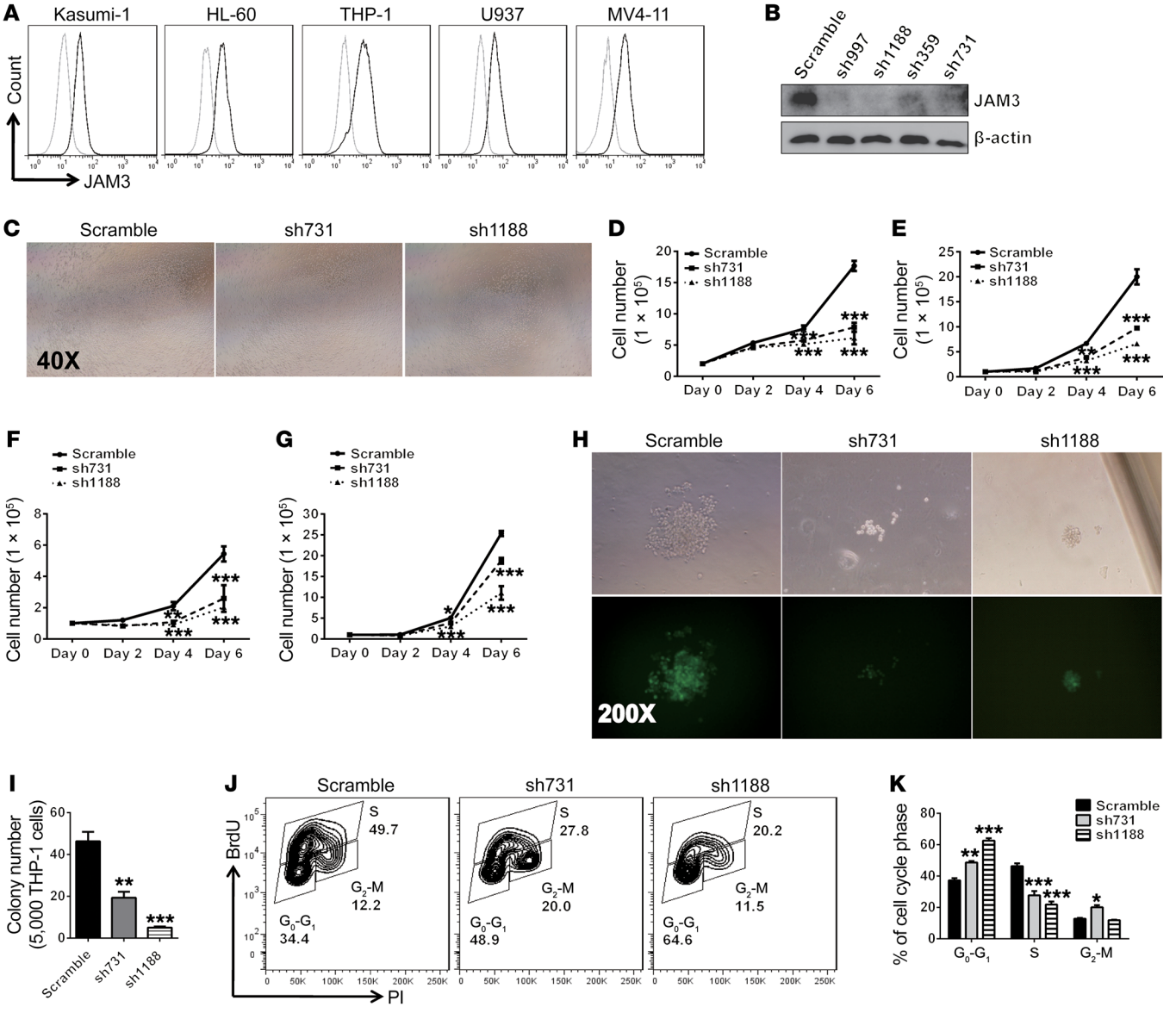

Figure 6. JAM3 is required for the proliferation of human leukemia cell lines. (**A**) Representative flow cytometric analysis of JAM3 expression on different leukemia cell lines including Kasumi-1 (M2), HL-60 (M3), THP-1 (M5), U937 (M5), and MV4-11 (M5). (Isotype control, gray line). (**B**) FLAG-tagged *JAM3* and shRNAs targeting *JAM3* (sh997, sh1188, sh359, and sh731) were cotransfected into 293T cells (1:4 ratio), followed by immunoblotting for JAM3. (**C**) Representative images of *JAM3*-knockdown (sh731 and sh1188) THP-1 cells after 6 days in culture. (**D**–**G**) The numbers of THP-1, U937, Kasumi-1, and HL-60 cells were counted at the indicated days after infection with the *JAM3*-targeting sh731 or sh1188 or scrambled shRNA ($n = 3$; $^*P < 0.05$, $^{**}P < 0.01$, $^{***}P < 0.001$, 2-way ANOVA followed by Bonferroni's post-test). (**H**) Representative images of colonies formed by the *JAM3*-knockdown (sh731 and sh1188) THP-1 cells after 9 days of culture in 1640 medium supplemented with 0.9% of methylcellulose and 10% of FBS. (**I**) Quantification of colony numbers in **H** ($n = 3$; $^{**}P < 0.01$, $^{***}P < 0.001$, 1-way ANOVA followed by Bonferroni's post-test). (**J**) Representative flow cytometric analysis of the cell cycle distribution in THP-1 cells targeted by sh731, sh1188, or scrambled shRNA, which was determined using BrdU incorporation. (**K**) Quantitative analysis of the cell cycle distribution results in **J** ($n = 3$; $^*P < 0.05$, $^{**}P < 0.01$, $^{***}P < 0.001$, 2-way ANOVA followed by Bonferroni's post-test). Experiments were conducted 3–5 times for validation.

[GEO] GSE42519 for normal hematopoiesis and GSE13159 for AML cells), which shows that *JAM3* expression level increases in AML with t(15;17) or AML with complex aberrant karyotype (AML complex) compared with HSCs or GMP cells, but not in AML with inv(16)/t(16;16), AML with t(8;21), or AML with t(11q23)/MLL (Supplemental Figure 7B). Consistently, in other RNA sequencing expression data of 9,736 tumors and 8,587 normal samples from the The Cancer Genome Atlas project (TCGA; https://tcga-data.nci.nih.gov/tcga) and the Genotype-Tissue Expression project (https://cancergenome.nih.gov/), *JAM3* expression is found to be significantly elevated in AML cells compared with that in normal control (Supplemental Figure 7C). Although the data for *JAM3* expression in MLL-AF9$^+$ AML are not available in these databases, we found that *JAM3* expression level in MLL-rearranged leukemia [t(11q23)/MLL] is similar to that in HSCs (Supplemental Figure 7B). However, it is possible that LICs from these different types of AMLs have higher levels of *JAM3* than that in HSCs, since current databases do not provide this information.

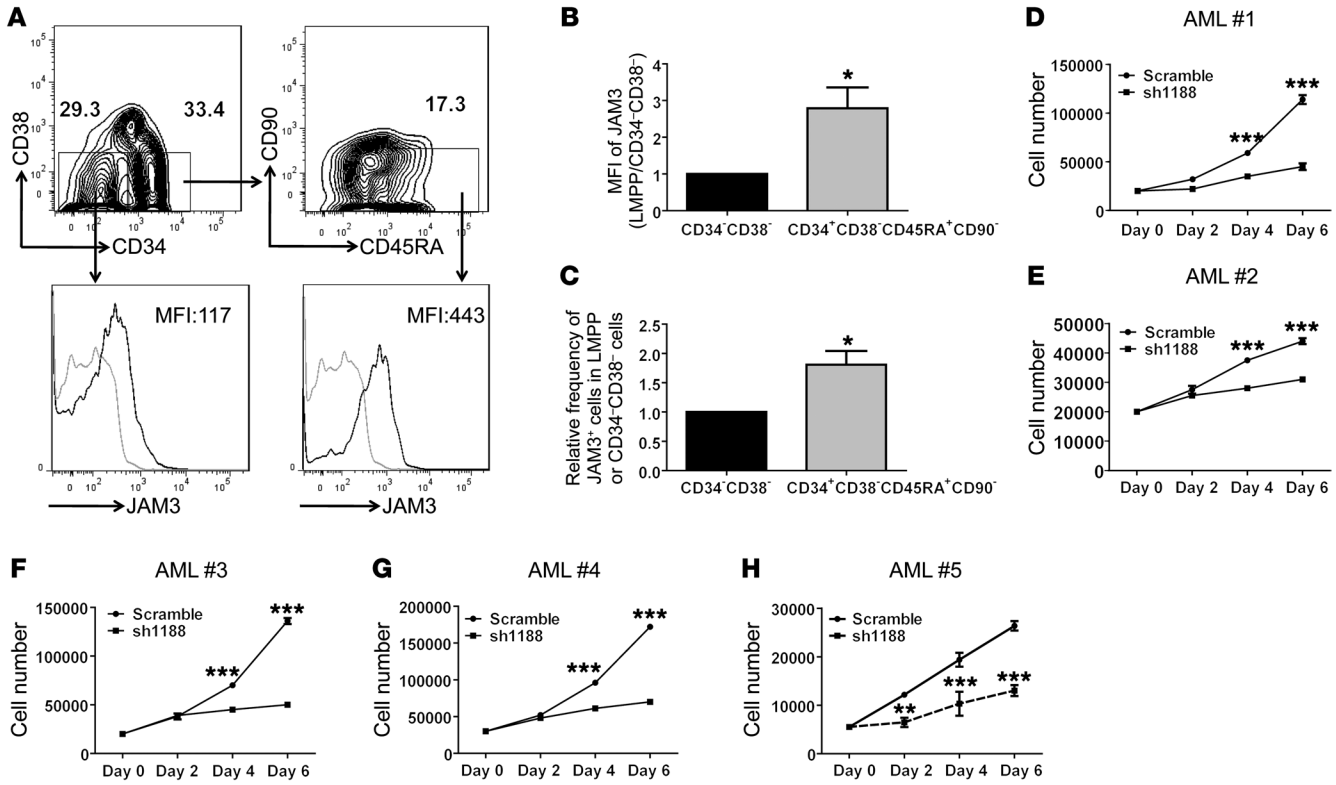

Figure 7. JAM3 supports the growth of human acute myeloid LICs. (**A**) Representative flow cytometric analysis of JAM3 expression on the immunophenotypic Lin⁻CD34⁺CD38⁻CD90⁻CD45RA⁺ LICs (LMPP cells) and CD34⁻CD38⁻ differentiated human AML cells (AML#7 in Supplemental Table 2). (**B**) Quantification of the MFIs for JAM3 expression on LMPP cells or CD34⁻CD38⁻ differentiated leukemia cells in **A** (AML#2, #5, #6, #8 in Supplemental Table 2; $n = 5$; $^*P < 0.05$, Student's t test). (**C**) Quantification of the relative frequency of JAM3⁺ cells in LMPP or CD34⁻CD38⁻ differentiated leukemia cells in **A** ($n = 5$; $^*P < 0.05$, Student's t test). (**D**–**H**) Cell numbers of 5 patient AML samples were counted at the indicated days after knockdown of *JAM3* by sh1188 or scrambled shRNA (AML#1–AML#5 in Supplemental Table 2; $n = 3$; $^{**}P < 0.01$, $^{***}P < 0.001$, 2-way ANOVA followed by Bonferroni's post-test). Experiments were conducted 3–5 times for validation.

Interestingly, it seems that the rates of point mutation and copy number variation (CNV) are relatively low in AML samples (0.03% and 0.12%, respectively), while the frequency of gene overexpression (8.14%) is much higher than point mutation and CNV (Supplemental Table 3), which is consistent with our findings that deletion of *Jam3* in murine LICs leads to a notably delayed leukemogenesis. More importantly, the *JAM3* expression level was inversely correlated with the overall survival of AML patients, showing that the lower expression level of *JAM3* in AML patients (0%–50%, top 50%) led to the much longer overall survival (Supplemental Figure 7D). Because it seems that not enough MLL-AF9 cases are available in the database for a similar plot for the overall survival, we showed a plot with all the MLL-rearranged AML cases (TCGA AML database, https://cancergenome.nih.gov/; accessed November 5, 2012), which showed that *JAM3* expression negatively regulates the overall survival of patients (Supplemental Figure 7E).

We thus knocked down *JAM3* in several human M2 (1 case, AML#4) and M5 AML samples (4 cases, AML#1, AML#2, AML#3, and AML#5) with or without MLL-AF9 fusion using sh1188 and found that the *JAM3*-knockdown CD34⁺ LICs from all the samples had a notable delayed growth ability, indicating that JAM3 is also required for the proliferation of human LICs (Figure 7, D–H). We believed that the reduction in number of primary AML cells was due to the G_1 cell cycle arrest (Supplemental Figure 7, F and G), which might further lead to the apoptosis during in vitro culture (Supplemental Figure 7, H and I). Meanwhile, we knocked down the *JAM3* expression in human cord blood CD34⁺ cells and revealed that the engraftment remained unchanged 2 months after transplantation (Supplemental Figure 7, J and K), indicating that JAM3 had no effect on the stemness maintenance of normal human stem progenitor cells, which was similar to what we found in murine HSCs. In summary, a working model is depicted in Supplemental Figure 7L, indicating that JAM3 interacts with LRP5 to activate the downstream PDK1/AKT pathway, followed by the downregulation of GSK3β and activation of β-catenin/CCND1 signaling to maintain the self-renewal ability and cell cycle entry of LICs. Conversely, JAM3 does not affect normal hematopoiesis. These findings support the notion that JAM3 serves as a functional LIC marker and may be an ideal target for eradicating LICs without affecting normal HSC functions.

Discussion

JAM3 is known to be involved in the regulation of cell migration or polarization of many cell types, including endothelial cells, neural stem cells, and spermatocytes. Herein, we have provided

several lines of unexpected evidence showing that JAM3 does not affect the migration, adhesion, or homing ability of LICs but that it is critical for the maintenance of the self-renewal ability of LICs through LRP5/PDK1/AKT/β-catenin/CCND1 signaling. These results suggest that JAM3 has different functions in different cell types, such as solid tumor cells or leukemia cells. Moreover, *Jam3* is highly expressed on LICs (Figure 1A) and is only enriched in approximately 30% of leukemia cells (but this population consists of approximately 5-fold more immunophenotypic LICs; Figure 1, B–D), indicating that JAM3 may be an ideal surface marker for the enrichment of functional LICs as exhibited by the dramatically extended survival times of *Jam3*-null leukemic mice in this study. It is also possible that JAM3 is enriched in other types of cancer stem cells (such as solid tumors) and has overwhelming influences on the cell fates of cancer stem cells.

In this study, we demonstrated that JAM3 directly interacts with LRP5 to enhance the PDK1/AKT pathway or inhibit GSK3β signaling to activate the downstream targets of β-catenin/CCND1, although the underlying details are not fully understood. To our knowledge, this is the first report showing that JAM3 is associated with LRP5, although which domain of JAM3 is involved in this interaction remains unknown. Mandicourt et al. have shown that serine 281 phosphorylation is critical for the establishment of tight junctions and cell polarity (39). It will be interesting to further explore whether the JAM3-LRP5 interaction is also dependent on serine 281 phosphorylation or whether other phosphorylation sites are required for JAM3's roles in leukemogenesis. Although LRP5 seems to be able to recruit both PDK1 and GSK3β to enhance the downstream β-catenin/CCND1 activities, our data show that constitutively active AKT signaling can partially rescue the loss of JAM3 function (Figure 5D), indicating that JAM3/LRP5/PDK1/AKT, but not JAM3/LRP5/GSK3β, control the β-catenin/CCND1 activities during leukemogenesis. Meanwhile, we also observed that the total protein levels of PDK1 and β-catenin were notably decreased in *Jam3*-null LICs, suggesting that JAM3/LRP5 signaling has additional roles in maintaining the stability of these proteins. More efforts are required to fully illustrate the underlying regulatory network of JAM3/LRP5/PDK1/AKT/β-catenin/CCND1 signaling.

JAM3 belongs to the immunoglobulin superfamily and is an important adhesion molecule with multiple functions. JAM3 may interact with other adhesion molecules, such as ITGB3, to regulate cell permeability (41) or adhesion/migration (39). We also demonstrated that JAM3 directly associates with LRP5, which may interact with ITGB3 or other surface molecules to trigger downstream signaling. Currently, JAM2 has been identified as a ligand for JAM3, and their interaction is important for the homing of human lymphoma cells to lymphoid organs (21). It will be interesting and important to know whether there are other ligands that have a much higher affinity for JAM3 than JAM2 does and whether the microenvironment also plays a role in JAM3-mediated leukemogenesis. A delineation of all the underlying extracellular interactions and intracellular signaling pathways induced by the JAM3 complex will benefit the development of cancer treatment strategies using anti-JAM3 antibodies or other small-molecule chemicals.

Currently, it is still controversial whether LICs reside in a quiescent cell population. Although many studies have indicated that quiescent LICs contribute to leukemia development (42–44), some studies have also suggested that there is a subset of actively cycling leukemia cells enriched for LIC activities (8). Cell cycle regulators, such as CDK6, may also differentially affect the maintenance of HSC or LIC activities (45). Consistently, our current data also show that another cell cycle regulator, CCND1, is important for the self-renewal of LICs. Loss of CCND1 leads to cell cycle arrest in G_1 phase, which dramatically delays leukemogenesis. Whether other cyclin proteins or cyclin-dependent kinases are also involved in the regulation of LIC stemness requires further investigation. It seems that tumor-initiating cells may not need to sustain a quiescent status compared with normal counterparts, although the underlying mechanisms remain largely unknown. Identification of other molecules that control the cell cycle status of LICs will further consolidate the notion that the quiescence and stemness of LICs are connected. In summary, we have revealed a novel role of JAM3 in sustaining the self-renewal capacity of LICs, but not HSCs, which is fine-tuned by the unexpected pathways of LRP5/PDK1/AKT/GSK3β/β-catenin/CCND1. JAM3 is highly enriched in functional LICs and may be an ideal therapeutic target for the elimination of LICs with immune strategies.

Methods

Mice. The *Jam3*-knockout mice with a C57BL/6 background were purchased from Mutant Mouse Resource and Research Centers. The CD45.1 mice were provided by Jiang Zhu at Ruijing Hospital, Shanghai, China. C57BL/6 CD45.2 and NOD-SCID mice were ordered from Shanghai SLAC Laboratory Animal Co. Ltd. and maintained at Animal Core Facility. All the animal experiments were approved by our institution and conducted under the Guideline for Animal Care at Shanghai Jiao Tong University School of Medicine.

Establishment and analysis of the murine AML model, rescue experiments, and competitive reconstitution analysis. A transplantable MLL-AF9–inducible murine AML model was established as previously described (9). Briefly, an MSCV-MLL-AF9-IRES-YFP–encoding plasmid (32) and a pCL-ECO packaging plasmid were transfected into 293T cells (ATCC) to produce retroviruses, followed by the infection of isolated WT and *Jam3*-null Lin^- fetal liver cells by 2 rounds of spin-oculation in the presence of 4 μg/ml Polybrene. Infected cells (2×10^5 to 3×10^5) were transplanted into lethally irradiated (10 Gy) C57BL/6 mice by retro-orbital injection. Serial transplantations were performed with 8,000 purified YFP^+ BM leukemia cells or 600 purified L-GMP cells of either primary or secondary recipient mice. In another case, 400,000 YFP^+ leukemia cells of primary recipients were transplanted into sublethally irradiated recipient mice for the evaluation of leukemia development. For the limiting dilution analysis, the indicated YFP^+ WT and *Jam3*-null MLL-AF9$^+$ BM cells (Supplemental Table 1) that were collected from secondary recipients were cotransplanted with 2×10^5 competitor cells into lethally irradiated recipient mice. The survival times were recorded to calculate LIC frequencies using L-Calc software from Stemcell Technologies. For establishing the M2 AML or B cell acute lymphoid leukemia model, MigR1-AML1-ETO9a-IRES-GFP– or pMXs-N-Myc-IRES-GFP–encoding plasmid was used to transform hematopoietic stem/progenitor cells (33, 34).

For the rescue experiments, the retroviral plasmid MSCV-Ccnd1-IRES-mCherry, lentiviral plasmid pCDH-EF1a-β-catenin^{CN}-T2A-mCherry (S37A) (constitutively phosphorylated at S552), or pCDH-EF1a-AKT^{CN}-T2A-mCherry (E17K) (constitutively phosphorylated

at T308; the pCDH-EF1a-T2A plasmid was provided by Chuanxin Huang, Shanghai Jiao Tong University School of Medicine) was cotransfected with pCL-ECO (2:1, for retroviral plasmid) or pMD2G and pSPAX2 (4:1:3, for lentiviral plasmid) into 293T cells (ATCC), and the resulting retroviral or lentiviral supernatant was collected for the infection of WT and *Jam3*-null leukemia cells, followed by transplantation into recipient mice as previously described (11). The expression levels of CCND1, β-catenin^{CN} (S552), and AKT^{CN} (T308) were further measured in WT, *Jam3*-null, and *Ccnd1/β-catenin^{CN}/AKT^{CN}*–overexpressing *Jam3*-null leukemia cells by immunoblotting.

For the competitive reconstitution analysis, a total number of 2×10^5 CD45.2 WT and *Jam3*-null donor BM cells were mixed with the same number of competitor BM cells and transplanted into 8- to 10-week-old lethally irradiated CD45.1 mice, followed by an analysis of the repopulation and multiple lineages of donor cells 4, 8, and 16 weeks after transplantation. Donor BM cells were further isolated from primary or secondary recipient mice 2–4 months after transplantation, followed by injection into the secondary and tertiary recipients, respectively.

Flow cytometric analysis. Flow cytometric analysis and cell cycle analysis were performed as previously described (9). In brief, the myeloid/lymphoid lineages and YFP$^+$Mac-1$^+$c-Kit$^+$ immunophenotypic LICs of WT and *Jam3*-null AML recipients were stained with anti–mouse Mac-1–APC, Gr-1–PE, CD3-APC, B220-PE, and c-Kit–PE monoclonal antibodies (eBioscience). Alternatively, lineage$^-$IL7R$^-$Sca-1$^-$c-Kit$^+$CD34$^+$FcR-II/III$^+$ immunophenotypic L-GMP cell frequencies were measured as previously described (32). Human Lin$^-$CD34$^+$CD38$^-$CD90$^-$CD45RA$^+$ LICs (LMPP cells) or cord blood Lin$^-$CD34$^+$CD38$^-$CD90$^+$CD45RA$^-$ HSCs and their normal LMPP cells were identified by antibodies against human Lin-eFluor450, CD34-FITC, CD38-PE-Cy7, CD90-PerCP-Cy5.5, and CD45RA-PE. The expression levels of JAM3 in mouse or human LICs (or leukemia cell lines) were examined by anti–mouse JAM3–PE and anti–human JAM3–APC (eBioscience). Cell cycle distribution of LICs was examined by Ki-67/Hoechst 33342 staining (BD Pharmingen), Pyronin Y/Hoechst 33342 staining, or BrdU incorporation analysis. To evaluate the apoptotic status, LICs were stained with anti–annexin V and 7-aminoactinomycin D (BD Pharmingen) according to the manufacturer's instructions. In some cases, Lin$^-$Sca-1$^+$c-Kit$^+$Flk2$^-$CD34$^-$ phenotypic LT-HSCs, Lin$^-$Sca-1$^+$c-Kit$^+$Flk2$^-$CD34$^+$ ST-HSCs, Lin$^-$Sca-1$^+$c-Kit$^+$Flk2$^+$CD34$^+$ MPP, Lin$^-$Sca-1$^-$c-Kit$^+$CD16/32$^+$CD34$^+$ GMP, and Lin$^-$Sca-1$^-$c-Kit$^+$CD16/32$^-$CD34$^+$ CMP progenitor cells were FACS-purified by staining with a biotinylated lineage cocktail (anti-CD3, anti-CD5, anti-B220, anti–Mac-1, anti–Gr-1, anti-Ter119; BD Pharmingen) followed by streptavidin-PE/Cy5.5, anti–Sca-1–FITC, anti–c-Kit–APC, anti-Flk2–PE, anti-CD34–eFluor450, and anti-CD16/32–PE (eBioscience). Detailed antibody information is listed in Supplemental Table 4.

Western blotting and coimmunoprecipitation. A combination of different plasmids of pLVX-strepII-JAM3-IRES-GFP, PLX304-blast-V5-PDK1, MSCV-HA-AKT, CMV-LRP5-FLAG, and their empty vectors were transfected into 293T cells, followed by the coimmunoprecipitation experiments for further detection of their interactions. In other cases, cell lysates of FACS-purified WT or *Jam3*-null YFP$^+$Mac-1$^+$c-Kit$^+$ LICs, *JAM3*-overexpressing THP-1 cells, and their control cells were electrophoresed on 8%–10% SDS polyacrylamide gels and transferred onto PVDF membranes (Millipore). The membranes were blocked with 5% nonfat milk, and reacted with indicated primary antibodies, followed by incubation with appropriate HRP-conjugated secondary antibodies. The primary antibodies were as follows: anti–human strepII (GenScript), anti–human V5 (Biodragon), anti–human FLAG (Cell Signaling Technology), anti-CCND1 (Cell Signaling Technology), anti-GSK3β (Cell Signaling Technology), anti–phospho-GSK3β (S9) (Abways), anti–β-catenin (Proteintech), anti–phospho–β-catenin (S552) (Cell Signaling Technology), anti-AKT (Santa Cruz Biotechnology), anti–phospho-AKT (T308) (Abways), anti-PDK1 (Bioworld), anti–phospho-PDK1 (S241) (Bioworld), anti-LRP5 (Cell Signaling Technology), and anti–β-actin (Calbiochem). Detailed antibody information is listed in Supplemental Table 4.

Microarray analysis and quantitative RT-PCR. WT and *Jam3*-null YFP$^+$Mac-1$^+$c-Kit$^+$ LICs were sorted by flow cytometry for the extraction of total RNA and subjected to microarray analysis at Bohao Biotechnology Co. Ltd., Shanghai, China. Gene ontology enrichment analysis was performed by the Bioconductor package topGO. A KEGG pathway enrichment analysis was conducted by the Bioconductor package GSEABase (https://bioconductor.org/packages/release/bioc/html/GSEABase.html) We have deposited the microarray data in the GEO repository (https://www.ncbi.nlm.nih.gov/geo/query/acc.cgi?acc=GSE109311), and the accession number GSE109311 was assigned. The selected target genes were further validated by quantitative RT-PCR analysis. Briefly, first-strand cDNA was reverse transcribed using M-MLV reverse transcriptase (Promega). PCR reactions were performed according to the manufacturer's instructions. In brief, 20-μl reactions with 2×ABI SYBR Green PCR Master Mix, primers, and cDNA were used for the evaluation of expression levels. The experiments were conducted in triplicate with an Applied Biosystems 7900HT PCR system. The mRNA level was normalized to the level of β-actin RNA transcripts. The primer sequences used are shown in Supplemental Table 5.

Colony-forming unit assays, Giemsa-Wright staining, and H&E staining. The indicated numbers of YFP$^+$Mac-1$^+$c-Kit$^+$ LICs of secondary recipient mice were seeded in methylcellulose (M3534, Stem Cell Technologies) according to the manufacturer's instructions. The same numbers of first plated leukemia cells were replated in methylcellulose for further analysis of the self-renewal ability of LICs. The numbers of colonies were counted 7–10 days after culture. Giemsa-Wright staining was performed with BM leukemia cells of secondary recipient mice, and the frequencies of blast cells were calculated according to their typical morphologies. Liver and spleen tissues were fixed in 4% paraformaldehyde and embedded in paraffin. Sections were stained with H&E for the analysis of the infiltration of leukemia cells.

Lentivirus construction, infection, and in vitro proliferation analysis. shRNAs targeting human *JAM3*, *LRP5*, or a scrambled shRNA were constructed using a lentiviral vector, PLKO1-GFP (sequences listed in Supplemental Table 5). Human JAM3 was subcloned into pLVX-IRES-GFP vector. Lentiviruses were produced using calcium phosphate transfection method with the packaging plasmids of pSPAX2 and pMD2G. Lentiviral supernatant was used to infect several human leukemia cell lines (Kasumi-1, HL-60, THP-1, and U937; ATCC) or primary AML cells (M2 or M5) from patients, followed by analysis for the signaling pathways or proliferation capabilities in vitro at indicated time points. Human primary AML cells were cultured in Stemspan basic medium (Stemcell Technologies) supplemented with 10 ng/ml human stem cell factor (SCF), 10 ng/ml human IL-3, and 10 ng/ml human IL-6 (all the growth factors were from PeproTech). In another experiment, *JAM3*-slienced human cord blood CD34$^+$ cells were

transplanted into NOD-SCID mice, followed by analysis for engrafted human cells 2 months after transplantation.

For the colony-forming assay of THP-1 cells, a total of 5,000 *JAM3*-knockdown THP-1 cells or control cells were cultured in 1640 medium supplemented with 0.9% of methylcellulose and 10% of FBS as previously described (46). Colonies were imaged and counted 7–10 days after plating.

Homing, migration, and adhesion analyses. Homing assays were performed as previously described (47, 48). Briefly, a total of 5×10^6 WT and *Jam3*-null BM leukemia cells of primary recipient mice were labeled with 5- (and 6-) CFSE and transplanted into lethally irradiated mice. Total $CFSE^+$ cells were examined in the BM and spleen 16 hours after injection by flow cytometry. In some cases, a total of 2×10^6 WT and *Jam3*-null $YFP^+Mac\text{-}1^+c\text{-}Kit^+$ LICs were transplanted into recipient mice, followed by analyses for the homed cells at 6, 12, and 18 hours after injection. In another experiment, WT and *Jam3*-null leukemia BM cells were directly transplanted into recipient mice through intratibial injection, followed by the measurement of YFP^+ leukemia cells in BM, peripheral blood, and spleen 2 weeks after transplantation.

Migration of $YFP^+Mac\text{-}1^+c\text{-}Kit^+$ LICs was evaluated using a Transwell with an 8-μm pore size (Corning Inc.). A total of 3×10^5 WT or *Jam3*-null LICs were seeded in the upper chamber in IMDM medium supplemented with 0.5% BSA, and 160 ng/ml SDF1 was added into IMDM medium with 0.5% BSA in the lower chamber. Cells in the lower chamber were counted 4 hours after culture (49). For cell adhesion assay, a total of 1×10^4 OP9-DL1 stromal cells (ATCC) were plated on a 96-well flat-bottom plate and cultured overnight, followed by incubation with 1×10^5 LICs for 1 hour. Plates were washed 3 times with PBS, and adhered cells were resuspended and calculated according to their different morphologies in cell size (50). For the coculture of LICs with stromal cells, 3×10^4 OP9-DL1 stromal cells were plated on a 24-well plate and cultured overnight, followed by incubation with 5×10^4 LICs for 2–3 days in Stemspan basic medium (Stemcell Technologies) supplemented with 10 ng/ml murine SCF, 10 ng/ml murine IL-3, and 10 ng/ml murine IL-6 (all the growth factors were from PeproTech) in either normoxic or hypoxic conditions (1% O_2) (51). Cells were counted and collected for subsequent analysis for the colony-forming assay.

Antibody treatment in leukemic mice. A total of 10,000 BM AML cells were isolated from primary leukemic mice and injected into recipient mice. Right after transplantation, 100 μg functional anti-JAM3 antibodies (catalog MCA5935XZ; clone CRAM-18 F26, Bio-Rad) (39, 40) or PBS were delivered into recipient mice via i.p. injection. Antibodies were given every other day for 8 days. The overall survival of recipient mice was recorded upon antibody treatment.

In silico analysis for clinical data. For the analysis of JAM3 expression in AML patients, data were extracted from the curated BloodSpot database (http://servers.binf.ku.dk/bloodspot/; GSE42519 for normal hematopoiesis and GSE13159 for AML cells), or RNA sequencing expression data of 9,736 tumors and 8,587 normal samples from the TCGA and GTEx projects (http://gepia.cancer-pku.cn/detail.php?gene=JAM3###). For the analysis of the relationship between JAM3 expression and overall survival, available survival data on 79 patients were obtained from the Leukemia Gene Atlas (http://www.leukemia-gene-atlas.org/LGAtlas/LGAtlas.html#newAnalysis), and data on 46 MLL-rearranged AML cases were obtained from the TCGA AML database (https://cancergenome.nih.gov/; accessed November 5, 2012). Patients were separated into 2 groups based on whether they had high (50%–100% or JAM3 high) or low (0%–50% or JAM3 low) JAM3 expression and then analyzed by Xena Kaplan-Meier plot (http://xena.ucsc.edu/survival-plots/).

Statistics. Data are represented as mean ± SEM. Unpaired 2-tailed Student's *t* test was used to assess 2 independent groups. In some cases, 1- or 2-way ANOVA followed by Bonferroni's post-test was conducted to assess the statistical significance of differences between multiple comparisons. The survival rates of the 2 groups were analyzed using a log-rank test. Statistical significance was set at *P* less than 0.05 ($^*P < 0.05$; $^{**}P < 0.01$; $^{***}P < 0.001$). Data were analyzed using GraphPad Prism 6 (GraphPad Software).

Study approval. BM mononuclear cells of AML samples from the patients following diagnostic work were kindly provided by the Department of Hematology at Xinhua Hospital, the First People's Hospital, or Tongren Hospital, Shanghai Jiao Tong University School of Medicine. Written informed consent was obtained from all of the patients, and all the procedures were approved by the Ethics Committee for Medical Research (IRB) at Shanghai Jiao Tong University School of Medicine.

Author contributions

YZ, FX, XL, ZY, and J. Zheng designed the experiments, performed the experiments, analyzed data, and wrote the paper. LX, LL, CC, HJ, X. Hao, X. He, FZ, HG, J. Zhu, and HB performed the experiments. CCZ and GQC provided reagents and helped with the experiments and the writing of the paper.

Acknowledgments

We appreciate Jiang Zhu at Ruijing Hospital, Shanghai, for his kindness in providing us with the CD45.1 mice. We thank Chuanxin Huang at Shanghai Jiao Tong University School of Medicine for his great help in providing the pCDH-EF1a-T2A plasmid. This work was supported by grants from the National Natural Science Foundation of China (NSFC; 81422001, 81570093, and 81370654), the 1000-Youth Elite Program, the National Basic Research Program of China (973Program, 2014CB965000; NO2015CB910403), the Natural Science Foundation of Shanghai (17ZR1415500), 1R01CA172268 (NIH), the Cancer Prevention and Research Institute of Texas (RP140402), the Taishan Scholar Immunology Program, and the innovative group of the NSFC (81721004, to GQC).

Address correspondence to: Junke Zheng, Department of Pathophysiology, Shanghai Jiao Tong University School of Medicine, 280 South Chongqing Road, Shanghai 200025, China. Phone: 86.21.63846590; Email: zhengjunke@shsmu.edu.cn.

1. Hutchinson L. Immunotherapy: CAR-modified T cells targeting CD19-curing the incurable. *Nat Rev Clin Oncol*. 2014;11(12):683.
2. Kochenderfer JN, et al. Chemotherapy-refractory diffuse large B-cell lymphoma and indolent B-cell malignancies can be effectively treated with autologous T cells expressing an anti-CD19 chimeric antigen receptor. *J Clin Oncol*. 2015;33(6):540–549.
3. Majeti R, et al. CD47 is an adverse prognostic factor and therapeutic antibody target on human acute myeloid leukemia stem cells. *Cell*. 2009;138(2):286–299.
4. Chao MP, et al. Therapeutic antibody targeting of CD47 eliminates human acute lymphoblastic leukemia. *Cancer Res*. 2011;71(4):1374–1384.

5. Zheng J, et al. Inhibitory receptors bind ANGPTLs and support blood stem cells and leukaemia development. *Nature*. 2012;485(7400):656–660.
6. Jin L, et al. Monoclonal antibody-mediated targeting of CD123, IL-3 receptor α chain, eliminates human acute myeloid leukemic stem cells. *Cell Stem Cell*. 2009;5(1):31–42.
7. Qiu S, et al. N-Cadherin and Tie2 positive $CD34^+CD38^-CD123^+$ leukemic stem cell populations can develop acute myeloid leukemia more effectively in NOD/SCID mice. *Leuk Res*. 2014;38(5):632–637.
8. Iwasaki M, Liedtke M, Gentles AJ, Cleary ML. CD93 marks a non-quiescent human leukemia stem cell population and is required for development of MLL-rearranged acute myeloid leukemia. *Cell Stem Cell*. 2015;17(4):412–421.
9. Gu H, et al. Sorting protein VPS33B regulates exosomal autocrine signaling to mediate hematopoiesis and leukemogenesis. *J Clin Invest*. 2016;126(12):4537–4553.
10. Wei J, et al. Microenvironment determines lineage fate in a human model of MLL-AF9 leukemia. *Cancer Cell*. 2008;13(6):483–495.
11. Fang X, et al. CD274 promotes cell cycle entry of leukemia-initiating cells through JNK/Cyclin D2 signaling. *J Hematol Oncol*. 2016;9(1):124.
12. Mandell KJ, Parkos CA. The JAM family of proteins. *Adv Drug Deliv Rev*. 2005;57(6):857–867.
13. Hao S, et al. JAM-C promotes lymphangiogenesis and nodal metastasis in non-small cell lung cancer. *Tumour Biol*. 2014;35(6):5675–5687.
14. Martìn-Padura I, et al. Junctional adhesion molecule, a novel member of the immunoglobulin superfamily that distributes at intercellular junctions and modulates monocyte transmigration. *J Cell Biol*. 1998;142(1):117–127.
15. Palmeri D, van Zante A, Huang CC, Hemmerich S, Rosen SD. Vascular endothelial junction-associated molecule, a novel member of the immunoglobulin superfamily, is localized to intercellular boundaries of endothelial cells. *J Biol Chem*. 2000;275(25):19139–19145.
16. Liang TW, et al. Vascular endothelial-junctional adhesion molecule (VE-JAM)/JAM 2 interacts with T, NK, and dendritic cells through JAM 3. *J Immunol*. 2002;168(4):1618–1626.
17. Gliki G, Ebnet K, Aurrand-Lions M, Imhof BA, Adams RH. Spermatid differentiation requires the assembly of a cell polarity complex downstream of junctional adhesion molecule-C. *Nature*. 2004;431(7006):320–324.
18. Stelzer S, et al. JAM-C is an apical surface marker for neural stem cells. *Stem Cells Dev*. 2012;21(5):757–766.
19. Leinster DA, et al. Endothelial cell junctional adhesion molecule C plays a key role in the development of tumors in a murine model of ovarian cancer. *FASEB J*. 2013;27(10):4244–4253.
20. Arcangeli ML, et al. The Junctional Adhesion Molecule-B regulates JAM-C-dependent melanoma cell metastasis. *FEBS Lett*. 2012;586(22):4046–4051.
21. Doñate C, et al. Homing of human B cells to lymphoid organs and B-cell lymphoma engraftment are controlled by cell adhesion molecule JAM-C. *Cancer Res*. 2013;73(2):640–651.
22. Praetor A, et al. Genetic deletion of JAM-C reveals a role in myeloid progenitor generation. *Blood*. 2009;113(9):1919–1928.
23. Bradfield PF, Nourshargh S, Aurrand-Lions M, Imhof BA. JAM family and related proteins in leukocyte migration (Vestweber series). *Arterioscler Thromb Vasc Biol*. 2007;27(10):2104–2112.
24. Ebnet K, et al. The junctional adhesion molecule (JAM) family members JAM-2 and JAM-3 associate with the cell polarity protein PAR-3: a possible role for JAMs in endothelial cell polarity. *J Cell Sci*. 2003;116(pt 19):3879–3891.
25. Reymond N, Garrido-Urbani S, Borg JP, Dubreuil P, Lopez M. PICK-1: a scaffold protein that interacts with Nectins and JAMs at cell junctions. *FEBS Lett*. 2005;579(10):2243–2249.
26. Santoso S, Orlova VV, Song K, Sachs UJ, Andrei-Selmer CL, Chavakis T. The homophilic binding of junctional adhesion molecule-C mediates tumor cell-endothelial cell interactions. *J Biol Chem*. 2005;280(43):36326–36333.
27. Santoso S, et al. The junctional adhesion molecule 3 (JAM-3) on human platelets is a counter-receptor for the leukocyte integrin Mac-1. *J Exp Med*. 2002;196(5):679–691.
28. Mirza M, et al. Coxsackievirus and adenovirus receptor (CAR) is expressed in male germ cells and forms a complex with the differentiation factor JAM-C in mouse testis. *Exp Cell Res*. 2006;312(6):817–830.
29. Lamagna C, Hodivala-Dilke KM, Imhof BA, Aurrand-Lions M. Antibody against junctional adhesion molecule-C inhibits angiogenesis and tumor growth. *Cancer Res*. 2005;65(13):5703–5710.
30. Doñate C, Vijaya Kumar A, Imhof BA, Matthes T. Anti-JAM-C therapy eliminates tumor engraftment in a xenograft model of mantle cell lymphoma. *J Leukoc Biol*. 2016;100(5):843–853.
31. Somervaille TC, Cleary ML. Identification and characterization of leukemia stem cells in murine MLL-AF9 acute myeloid leukemia. *Cancer Cell*. 2006;10(4):257–268.
32. Krivtsov AV, et al. Transformation from committed progenitor to leukaemia stem cell initiated by MLL-AF9. *Nature*. 2006;442(7104):818–822.
33. Yan M, et al. A previously unidentified alternatively spliced isoform of t(8;21) transcript promotes leukemogenesis. *Nat Med*. 2006;12(8):945–949.
34. Sugihara E, et al. Ink4a and Arf are crucial factors in the determination of the cell of origin and the therapeutic sensitivity of Myc-induced mouse lymphoid tumor. *Oncogene*. 2012;31(23):2849–2861.
35. Chen BB, et al. F-box protein FBXL2 targets cyclin D2 for ubiquitination and degradation to inhibit leukemic cell proliferation. *Blood*. 2012;119(13):3132–3141.
36. Arrate MP, Rodriguez JM, Tran TM, Brock TA, Cunningham SA. Cloning of human junctional adhesion molecule 3 (JAM3) and its identification as the JAM2 counter-receptor. *J Biol Chem*. 2001;276(49):45826–45832.
37. Lamagna C, et al. Dual interaction of JAM-C with JAM-B and α(M)β2 integrin: function in junctional complexes and leukocyte adhesion. *Mol Biol Cell*. 2005;16(10):4992–5003.
38. Deng M, et al. A motif in LILRB2 critical for Angptl2 binding and activation. *Blood*. 2014;124(6):924–935.
39. Mandicourt G, Iden S, Ebnet K, Aurrand-Lions M, Imhof BA. JAM-C regulates tight junctions and integrin-mediated cell adhesion and migration. *J Biol Chem*. 2007;282(3):1830–1837.
40. Johnson-Léger CA, Aurrand-Lions M, Beltraminelli N, Fasel N, Imhof BA. Junctional adhesion molecule-2 (JAM-2) promotes lymphocyte transendothelial migration. *Blood*. 2002;100(7):2479–2486.
41. Li X, et al. JAM-C induces endothelial cell permeability through its association and regulation of β3 integrins. *Arterioscler Thromb Vasc Biol*. 2009;29(8):1200–1206.
42. Lechman ER, et al. miR-126 regulates distinct self-renewal outcomes in normal and malignant hematopoietic stem cells. *Cancer Cell*. 2016;29(2):214–228.
43. Takeishi S, Matsumoto A, Onoyama I, Naka K, Hirao A, Nakayama KI. Ablation of Fbxw7 eliminates leukemia-initiating cells by preventing quiescence. *Cancer Cell*. 2013;23(3):347–361.
44. Ito K, et al. PML targeting eradicates quiescent leukaemia-initiating cells. *Nature*. 2008;453(7198):1072–1078.
45. Scheicher R, et al. CDK6 as a key regulator of hematopoietic and leukemic stem cell activation. *Blood*. 2015;125(1):90–101.
46. Sasaki S, et al. Cloning and expression of human B cell-specific transcription factor BACH2 mapped to chromosome 6q15. *Oncogene*. 2000;19(33):3739–3749.
47. Zheng J, Huynh H, Umikawa M, Silvany R, Zhang CC. Angiopoietin-like protein 3 supports the activity of hematopoietic stem cells in the bone marrow niche. *Blood*. 2011;117(2):470–479.
48. Huynh H, et al. IGF binding protein 2 supports the survival and cycling of hematopoietic stem cells. *Blood*. 2011;118(12):3236–3243.
49. Voermans C, van Heese WP, de Jong I, Gerritsen WR, van Der Schoot CE. Migratory behavior of leukemic cells from acute myeloid leukemia patients. *Leukemia*. 2002;16(4):650–657.
50. Arcangeli ML, et al. JAM-B regulates maintenance of hematopoietic stem cells in the bone marrow. *Blood*. 2011;118(17):4609–4619.
51. Cipolleschi MG, Dello Sbarba P, Olivotto M. The role of hypoxia in the maintenance of hematopoietic stem cells. *Blood*. 1993;82(7):2031–2037.